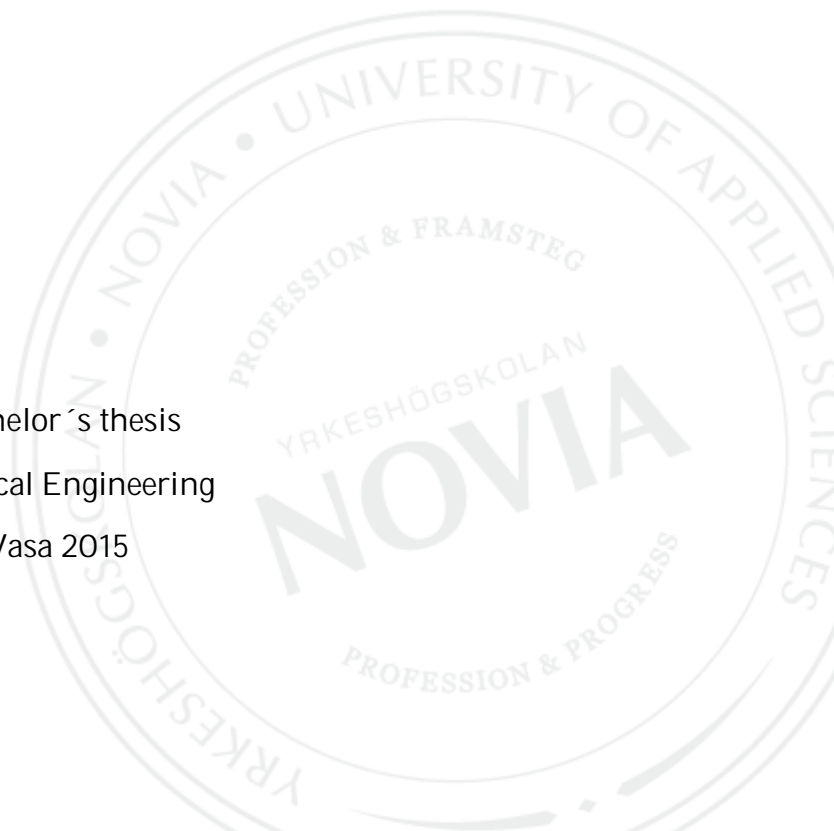




Knock Sensor Failure Behavior on Wärtsilä Gas Engines

Thomas Dahl

Bachelor's thesis
Electrical Engineering
Vasa 2015



This is an official version of the thesis.

Chapters containing confidential information have been removed from this thesis version.

BACHELOR'S THESIS

Author: Thomas Dahl
Degree Programme: Electrical Engineering
Specialization: Automation Technology
Supervisor: Roger Mäntylä

Title: *Knock sensor failure behaviour on Wärtsilä gas engines*

Date 9.4.2015 Number of pages 62

Summary

This thesis contains investigations concerning the effect temperature has on the knock measurement systems used on Wärtsilä gas engines. Testing of new knock sensors is also a part of the thesis. The objective of the thesis is to find out the cause why the knock sensor failure detection system is temperature sensitive in certain cases, and to find a solution to the problem.

The thesis contains information concerning engine knocking and how it is measured, and also a short introduction to gas engines and knock sensors. The physical phenomenon behind the functional principle of a knock sensor is also explained.

A Root Cause analysis was performed to get an overall view of the system and the test results.

Language: English Key words: knock, piezoelectric effect, insulation resistance

The thesis is available in either the web library Theseus.fi or in Tritonia Academic Library, Vaasa.

EXAMENSARBETE

Författare: Thomas Dahl
Utbildningsprogram: Elektroteknik
Inriktningalternativ: Automationsteknik
Handledare: Roger Mäntylä

Titel: *Felbeteende hos knackgivare på Wärtsiläs gasmotorer*

Datum 9.4.2015 Sidantal 62

Abstrakt

Detta examensarbete innehåller undersökningar om temperaturens inverkan på de knackmätningssystem som används på Wärtsiläs gasmotorer. Också testning av andra knackgivartyper finns med i examensarbetet. Målet var att hitta orsaken till att knackgivardiagnostiksystemet är temperaturkänsligt och att hitta en lösning på problemet. Dokumentet innehåller information som berör motorknack och hur detta mäts, samt kortfattat om gasmotorer och knackgivare. Fysiken som behövs för att förstå knackgivarnas funktion finns också förklarad.

En ”Root Cause-analys” har gjorts för att få en helhetsbild av systemet och alla resultat från testerna.

Språk: engelska Nyckelord: knack, piezoelektrisk effekt, isolationsresistans

Examensarbetet finns tillgängligt antingen i webbiblioteket Theseus.fi eller på Tritonia, Vasa ventenskapliga bibliotek.

OPINNÄYTETYÖ

Tekijä:	Thomas Dahl
Koulutusohjelma:	Sähkötekniikka
Suuntautumisvaihtoehto:	Automaatiotekniikka
Ohjaajat:	Roger Mäntylä

Nimike: Nakutusanturin vikadiagnostikkajärjestelmän käyttäytyminen Wärtsilän kaasumoottoreissa.

Päivämäärä 9.4.2015 Sivumäärä 62

Tiivistelmä

Tässä opinnäytetyössä on tutkittu miten lämpötila vaikuttaa nakutusjärjestelmään, jota käytetään Wärtsilän kaasumoottoreissa. Uusien nakutusanturien testaus on myös osa opinnäytetyötä. Opinnäytetyön tavoitteena oli löytää syy miksi nakutusanturien vikadiagnostikkajärjestelmä on lämpötilaherkkä ja löytää ratkaisu tähän ongelmaan. Opinnäytetyö sisältää tietoa mottorin nakutuksesta ja siitä kuinka se mitataan, sekä lyhyt esittely kaasumoottoreista ja nakutusantureista. Nakutusanturin toiminnan taustalla olevat fysikaaliset ilmiöt on myös selitetty. Syy-seuraus-analyysi tehtiin, jotta saataisiin parempi kokonaiskuva järjestelmästä ja tehdyistä testeistä.

Kieli: Englanti Avainsanat: nakutus, piezosähköinen vaikutus, eristysresistanssi

Opinnäytetyö on saatavissa web kirjastossa Theseus.fi tai Tritoniassa, Vaasa tieteellinen kirjasto.

Contents

Abbreviations.....	1
1 Introduction	2
1.1 Objectives	2
1.2 Organization.....	2
1.2.1 Ship Power	2
1.2.2 Power Plants	3
1.2.3 Services	3
2 Theory	3
2.1 Wärtsilä gas fuel engines.....	3
2.1.1 Gas engine types	4
2.1.2 Gas engine control systems.....	4
2.1.3 WECS 8000 modules.....	5
2.1.4 UNIC C3 modules	6
2.2 Engine knocking.....	7
2.2.1 Reasons for knocking.....	7
2.2.2 Effects of knocking.....	8
2.3 Knock sensors	8
2.3.1 Combustion pressure sensor.....	8
2.3.2 Mechanical Piezo sensors	9
2.3.3 Functional principle of a Piezo knock sensor.....	9
2.3.4 Bosch knock sensors.....	9
2.3.4.1 Specifications	11
2.3.4.2 Design	11
2.4 Piezoelectric effect	12
2.4.1 Applications	12
2.4.2 Direct and inverse piezoelectric effect.....	13

2.4.2.1 Direct piezoelectric effect	13
2.4.2.2 Electromechanical effect (inverse piezoelectric effect).....	13
2.4.3 Polarization.....	14
2.4.4 Mathematical description	17
2.4.5 Usage temperatures of piezoceramic materials	18
2.5 Pyroelectric effect	18
2.6 Knock measurement and sensor failure detection.....	20
2.6.1 Knock measurement	20
2.6.2 Sensor failure detection.....	22
2.6.2.1 Knock sensor replacement circuit.....	24
2.6.2.2 Sensor failure diagnostic circuit	24
2.7 Root cause analysis theory.....	25
2.7.1 Realitycharting process.....	25
3 Tests	28
3.1 General information	28
3.2 The initial problem	28
3.3 Heat cabinet	29
3.4 KS1 heat test with WECS 8000.....	30
3.4.1 Test results	30
3.5 KS1 drying test.....	31
3.5.1 Different drying times.....	33
3.5.2 Drying time	34
3.5.3 Temperature test 2 weeks after drying.....	35
3.5.4 Mounting torque test.....	37
3.5.5 Pyro-electric effect proof	38
3.6 Insulation resistance test.....	39
3.6.1 Test results	39
3.7 Knock diagnostic system simulation.....	42

3.7.1 Knock sensor replacement circuit.....	42
3.7.2 Simulation results	42
3.8 Engine block potential influence.....	44
3.9 Engine block potential tests	46
3.9.1 WECS 8000.....	46
3.9.2 UNIC C3	46
3.9.3 UNIC 2.....	46
3.10 Vibration tests	46
3.10.1 WECS 8000.....	46
3.10.2 UNIC C3	46
3.10.3 UNIC 2.....	46
4 Root Cause Analysis	47
4.1 Incident report.....	47
4.2 Reality Charting Possible Solutions Report	48
1.1 Realitychart.....	50
5 Results	51
6 Discussion.....	53
Bibliography	54

Abbreviations

WECS	Wärtsilä Engine Control System
UNIC	Unified Control
BMEP	Break Mean Even Pressure
KSFD	Knock Sensor Failure detection
DSP	Digital Signal Processing
CCM	Cylinder Control Module
MCM	Main Control Module
IOM	Input Output Module
LDU	Local Display Unit
ESM	Engine Safety Module
WCD	Wärtsilä Coil Driver
SG	Spark Ignited Gas
DF	Dual Fuel
GD	Gas Diesel
RCA	Root Cause Analysis

1 Introduction

1.1 Objectives

The primary goal of the thesis work is to identify and map how ambient conditions affect the output signal from the knock sensors used on Wärtsilä gas engines. The target is also to find working solutions on how to bypass or compensate for the effect of the signal fluctuations associated with the different ambient conditions.

The secondary goal is to scan the market for alternative sensors or solutions available that could be implemented on existing engines. Currently there are three different generations of automation systems in use on Wärtsilä engines, and the study must take into account how each system is affected.

1.2 Organization

Wärtsilä is a global leader in complete lifecycle power solutions for marine and energy markets. By emphasising technological innovation and total efficiency, Wärtsilä maximizes the environmental and economic performance of the vessels and power plants of its customers. In 2013, Wärtsilä's net sales totalled EUR 4.7 billion with approximately 18,700 employees. The company has operations in more than 200 locations in nearly 70 countries around the world. Wärtsilä is listed on NASDAQ OMX Helsinki, Finland.

1.2.1 Ship Power

Wärtsilä enhances the business of its marine and oil & gas industry customers by providing products and integrated solutions that are safe, environmentally sustainable, efficient, flexible, and economically sound. The solutions are developed based on customers' needs and include products, systems and services.

1.2.2 Power Plants

Wärtsilä Power Plants is a leading global supplier of flexible base load power plants of up to 600 MW operating on various gaseous and liquid fuels. The product portfolio includes solutions for peaking, reserve and load-following power generation, as well as for balancing intermittent power production. Wärtsilä Power Plants also provides LNG terminals and distribution systems. As of 2014, Wärtsilä has 55 GW of installed power plant capacity in 169 countries around the world.

1.2.3 Services

Wärtsilä Services supports its customers throughout the lifecycle of their installations by optimising efficiency and performance. The Service department provides services for both energy and marine markets. [1]

2 Theory

2.1 Wärtsilä gas fuel engines

Wärtsilä has several different types of gas-fuel engines, types which only run on gas like *SG* engines, or *DF* and *GD* engines which can run on either liquid fuels or gas.

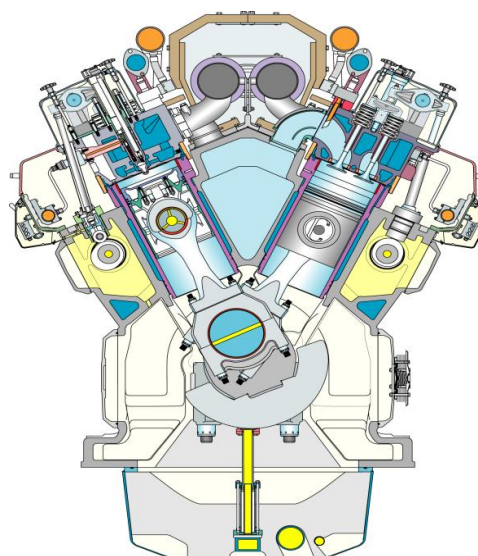


Figure 1 - 34SG engine [2]

Gas engines run with so-called *lean burn combustion* (not the GD engine). This means that the air/fuel ratio (λ) on gas engines is approximately $\lambda 2$, compared to a diesel engine for which the ratio is $\lambda 1$. This makes the gas engines produce less emissions and the efficiency of the engines is increased.

Figure 2 shows the operating window for gas engines. Here the benefits of a gas engine, compared to a diesel engine, can easily be seen. As the air/fuel ratio increases, the NO_x

values decrease and the thermal efficiency increases. A higher BMEP (Break Mean Effective Pressure) can also be achieved when the lambda value is increased. The challenge that comes with gas engines is a narrower operating window, which requires higher accuracy on actuators and control system. [2]

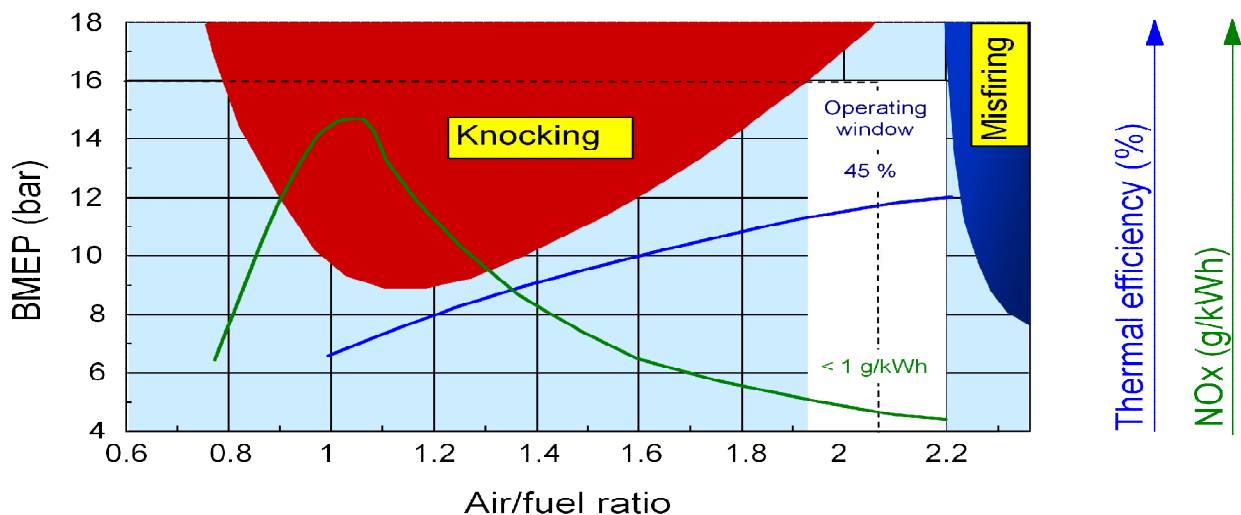


Figure 2 - Lean burn combustion [2]

2.1.1 Gas engine types

The two most common gas engine types manufactured by Wärtsilä today are:

SG (Spark-ignited Gas)

Low pressure gas engine.

DF (Dual Fuel)

Can run on both liquid fuel and low pressure gas.

2.1.2 Gas engine control systems

SG and DF engines have three different generations of control systems in use today and development of the fourth generation is currently ongoing.

The systems are:

WECS 3000

The first control system developed for SG and DF engines. Introduced in 1993 on gas engines.

WECS 8000

New hardware and new software design compared to WECS3000. Introduced in 1998.

UNIC C3

The current generation of control system for gas engines. The first control system with hardware completely designed by Wärtsilä. Production started in 2002.

UNIC2

The newest control system which is estimated to be taken in production on some pilot engines during 2015.

2.1.3 WECS 8000 modules

The WECS 8000 engine control system consists of the following modules:

MCM-700 - Main control module

Main control module, handles the main functions such as starting/stopping and speed measuring on the engine.

CCM10 - Cylinder controller module

Controls cylinder specific functions as exhaust gas temperature measurements, knock measuring and fuel injection for each cylinder.

ESM-10 - Engine safety module

ESM handles safety functions on the engine. ESM is an independent safety system for the engine with standardized solutions - its hardware and working principles are common for all engine applications and it uses unified marine and power plant solutions. The ESM provides a standardized stop circuitry for all actions and a standard interface to the engine control system and external systems with a predefined setting. The ESM also handles speed measuring and other similar functions.

LDU-10 – Local display unit

LDU (Local Display Unit) is a microprocessor-based display and Ethernet gateway unit adapted for Wärtsilä applications. The LDU-10 acts as an operator interface and as a communication interface to other networks.

WCD-10 *Wärtsilä coil driver*

Module used for spark plug ignition. Used on SG engines only, performs ignition to up to 10 cylinders. Capacity to perform one to six sparks per event to each spark plug (multispark). [3]

2.1.4 UNIC C3 modules

The UNIC engine control system comprises the following modules:

MCM-11 *Main Control Module*

The MCM is the main module of the engine and it controls among other things starting and stopping of the engine. The MCM also controls many of the other modules in the UNIC system.

CCM-20 *Cylinder Control Module*

As implied by the name, CCM handles functions related to cylinders. It controls fuel injection and cylinder specific measurements. One CCM can handle injection for up to three cylinders simultaneously and can act as a backup unit for another three cylinders. The CCM is also capable of functioning in limp mode if the CAN buses fail or if the MCM fails.

IOM-10 *Input Output Module*

The IOM-10 is a universal, configurable, microprocessor-based data acquisition unit. It has a variety of flexible analogue and digital measuring channels for different applications. Two analogue outputs and eight digital outputs are also provided.

ESM-20 *Engine Safety Module*

The ESM is an important module, if not the most important. It handles functions related to the safety of the engine. Also related to the engine safety, the module handles speed measuring and monitoring. Other functions include e.g. monitoring of the lube oil pressure and the cooling water temperature.

LDU-20 Local Display Unit

LDU-20 is a microprocessor-based display and Ethernet gateway unit adapted for Wärtsilä applications. The LDU-20 acts as an operator interface and as a communication interface to other networks. LDU-20 is the next LDU version after LDU-10. [3, 4]

2.2 Engine knocking

“Knock is the name given to the noise which is transmitted through the engine structure when essentially spontaneous ignition of a proportion of the end-gas ahead of the propagating flame front occurs”. The fuel-air mixture is meant to be ignited by a spark plug only, and at a precise point in the piston's stroke. Knock occurs when the peak of the combustion process no longer occurs at the optimum moment for the four-stroke cycle. The shock wave creates the characteristic metallic "pinging" sound, and cylinder pressure increases dramatically. Effects of engine knocking can be inconsequential or completely destructive. [5]

2.2.1 Reasons for knocking

Knocking is a result of temperature, pressure and time. If, for instance, the temperature and pressure of the end gases reach the threshold for self-ignition before the flame front initiated by the spark has had time to propagate to the cylinder walls, a knock will occur./4/

Several factors can cause knocking, for example:

- High compression of air-fuel mixture
- High temperature of cylinder wall
- Glowing combustion (engine oil) residues in the cylinder
- Methane number of the fuel too low
- Inhomogeneous air-fuel mixture
- Engine speed and engine load
- Ignition timing too early

2.2.2 Effects of knocking

Knocking has many different effects on engines. These range from mechanical wear to an actual damaging effect on different parts on the engine.

When knocking occurs, the cylinder pressure can be remarkably higher compared to the pressure at normal combustion. The same applies for the temperature in the cylinders. This leads to an increased risk of engine seizure. Engine parts may suffer from mechanical deformation because of knocking, due to the increased pressure and temperature inside the cylinder chamber. Engine efficiency is also something that is directly affected by knocking. Comparing an engine under normal running conditions with a heavily knocking engine shows that engine efficiency drops several percent. Effects of engine knocking range from inconsequential (light knocking) to completely destructive (heavy knocking). [4, 6]

Direct effects of prolonged knocking includes:

- Damaged cylinder heads and cylinder head gaskets
- Piston seizure
- Melting pistons and valves
- Increasing abrasion on bearings
- Higher fuel consumption
- Higher level of exhaust gas emissions.

2.3 Knock sensors

Knock can be measured in several different ways. Wärtsilä uses two different methods which include two different sensor types. One method is to measure the cylinder peak pressure and in that way detect knocking. The other way is a detection system which is using mechanical piezo knock sensors. [6]

2.3.1 Combustion pressure sensor

A direct approach is to analyze the combustion pressure-curve. In this approach the sensors measure the pressure inside the combustion chamber of a running engine. This approach provides the best signal to analyze and it is used on some Wärtsilä engines. However, the direct approach is not available on all engines, as the sensor cost is relatively high and each cylinder requires its own sensors. [4]

2.3.2 Mechanical Piezo sensors

This type of knock sensor is a structure-borne noise microphone and transforms the engine vibrations caused by normal combustion and caused by knocking combustion to electrical signals. It measures the structure-borne vibrations on the cylinder that occur at uncontrolled combustion. As a result of the forces generated by the vibrations in the engine the piezo-elements in the sensors generate a voltage that can be measured. [4] This is the type of sensor which will be tested in this report.

2.3.3 Functional principle of a Piezo knock sensor

The functionality of this sensor type is based on the piezoelectrical effect which is described in the *piezoelectric effect* chapter in this report.

A sensor consists of three main parts: a piezoceramic disc, a seismic mass and contact discs placed on each side of the piezo disc. The inertia of the seismic mass causes changing pressure forces on the Piezo ceramic disc corresponding to the acceleration. This rhythmical increase and decrease of the pressure force causes a movement of the electrical charges in the ceramic disc (Piezo effect) which can be conducted by the contact discs and be measured as a voltage signal. [3]

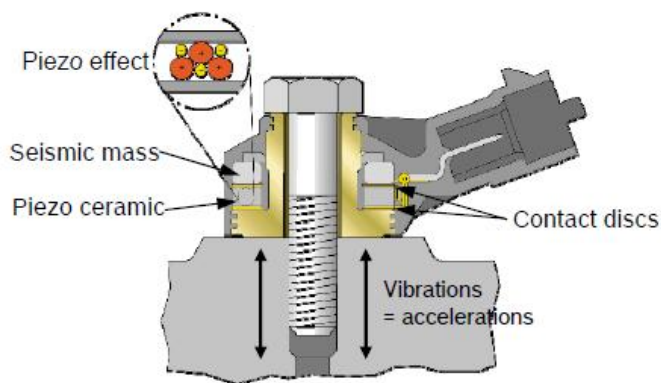


Figure 3- Functional principle of a knock sensor [6]

2.3.4 Bosch knock sensors

The sensors which are used by Wärtsilä and investigated in this report are manufactured by Bosch. Two models are investigated in this report, the KS1 model and the KS4 model.



Figure 4 - KS1 sensor

The knock sensor type which is presently used on Wärtsilä engines is the KS1 type. Nowadays Bosch is manufacturing this model for only a few customers, including Wärtsilä. The model was developed about 25 years ago.



Figure 5 - KS4 sensor

KS4

KS4 is developed from the KS1 sensor and is now the knock sensor that Bosch manufactures most of. Samples of this model were ordered with the purpose to test if this model would be suitable and have better insulation resistance than the KS1 sensors.

The main differences between the KS1 and the KS4 sensors are:

- Changed piezomaterial from Sonox P4 to Sonox P8
- Smaller housing diameter
- Threaded ring replaced by crimps
- Changed housing design

KS4 with new molding material

A KS4 sensor is a model with a new type of molding material that is less temperature sensitive. The heat stabilizer in the old molding material used on previous sensors was based on metal salts, which results in a decreasing insulation resistance due to moisture ingress. The heat stabilizer in the new molding material is metal salt free and is not as moisture sensitive as the old material. [Alfred Glatz, personal communication, 14.2.2015]

2.3.4.1 Specifications

These specifications are valid for knock sensors with brass support sleeve.

	KS1	KS4
Sensitivity (5 kHz, 190 pF load capacitance)	26 ± 8 mV/g	30 ± 6 mV/g
Linearity from 5...20 kHz	$\pm 15\%$	$\pm 10\%$
Frequency range	3...22 kHz	3...25 kHz
Main resonance frequency	> 30 kHz	> 30 kHz
Insulation resistance	> 1 M Ω	> 1 M Ω
Sensor capacitance	800...1600 pF	950...1350 pF
Operating temperature: silver/gold plated	-40...150 °C	-40...150 °C
Temperature dependency	< -0.06 mV/g K	< -0.04 mV/g K

[6]

2.3.4.2 Design

The following figure is an exploded view of a Bosch KS4- knock sensor.

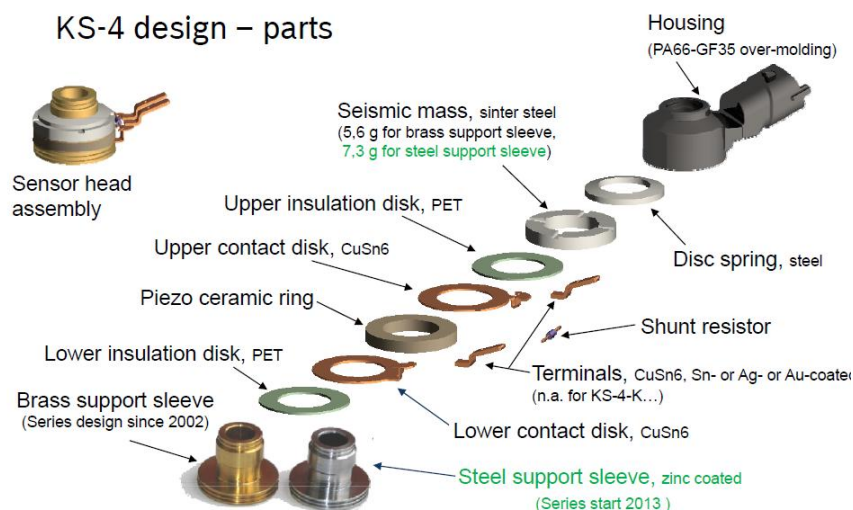


Figure 6 - Design of a KS4 knock sensor [6]

2.4 Piezoelectric effect

Piezoelectricity can shortly be explained as the electric charge that accumulates in certain solid materials in response to applied mechanical stress (direct piezoelectric effect). The word piezoelectricity means electricity resulting from pressure. It is derived from the Greek piezo or piezein ($\pi\acute{\epsilon}\zeta\epsilon\iota\nu$), which means to squeeze or press.

The piezoelectric effect is a reversible process, in which materials exhibiting the direct piezoelectric effect also exhibit the reverse piezoelectric effect. This means that an applied electric field causes a mechanical strain in the piezomaterial. [7]

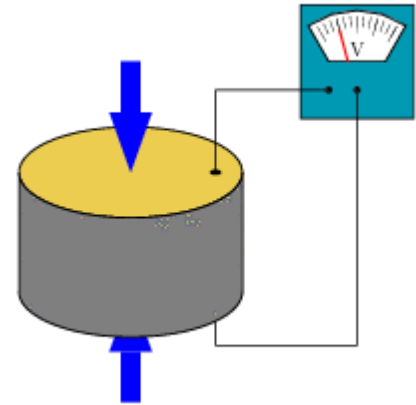


Figure 7 - Piezoelectric effect principle [7]

2.4.1 Applications

Piezo technology is used in high-end technology markets, such as medical technology, mechanical and automotive engineering or semiconductor technology, but is also present in everyday life, for example as generator of ultrasonic vibrations in a cleaning bath for glasses and jewellery or in medical tooth cleaning.

Piezo actuator technology has also gained acceptance in automotive technology, because piezo-controlled injection valves in combustion engines reduce the transition times and significantly improve the smoothness and exhaust gas quality. Several models of piezo-sensors are also occurring in the automotive technology and in the industry.

Piezo-based ultrasonic sensors are used as park distance control and monitor the heartbeats of babies prior to birth. Ultrasound is defined as sound at frequencies above the human hearing frequency range, i.e. starting from around 16 kHz. Industry, medical technology and research use this frequency range for many purposes. Applications range from distance measurement and object recognition, filling level or flow rate metering, to ultrasonic welding or bonding, high-resolution material tests, and medical diagnostics and therapy.

[8]

2.4.2 Direct and inverse piezoelectric effect

The piezoelectric effect can be split up into two parts depending on if a voltage is applied or produced.

2.4.2.1 Direct piezoelectric effect

This phenomenon converts mechanical energy to electrical energy. This means that when an external mechanical force is applied on the piezo material an electric charge will be produced by the material. Piezomaterials generally have a charge balance which means that the negative and the positive internal charges in the material nullify each other. When this charge balance is disrupted by an external mechanical force, the energy is transferred by electric charge carriers in the material. This is creating a surface charge which can be collected via electrodes placed on opposite sides of the piezo material. Changing the direction of deformation (pulling the material instead of squeezing it) will reverse the direction of the collected electrical current.

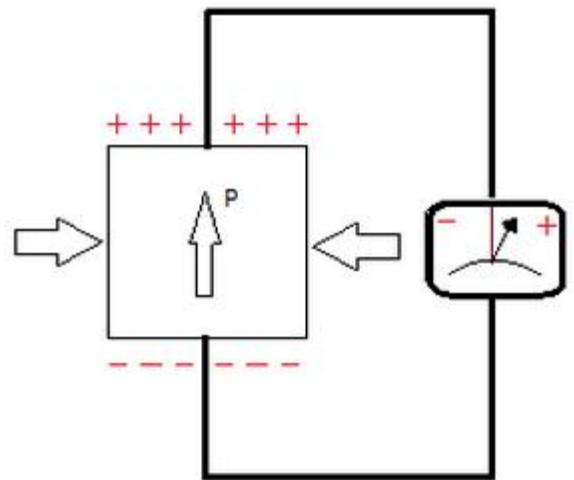


Figure 8 -Piezoelectric effect [17]

2.4.2.2 Electromechanical effect (inverse piezoelectric effect)

In opposite to the direct piezoelectric effect that converts a mechanical force to an electrical current, the inverse piezoelectric effect converts an electrical field applied on the material to mechanical force. This phenomenon arises when an electric field is applied over a piezo material. If an AC voltage is applied on the material, the deformation of the material will occur with the same frequency as the AC voltage. [9]

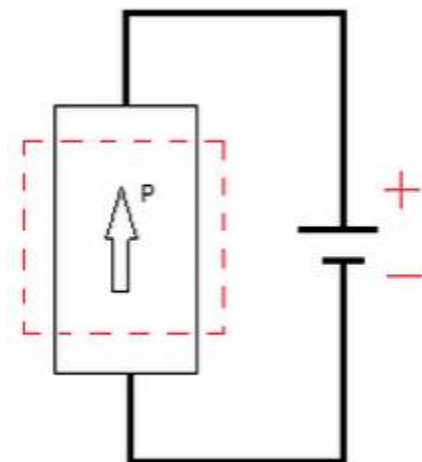


Figure 9 - Electromechanical effect [17]

2.4.3 Polarization

A presumption for a piezoelectrical and pyroelectrical material is that the material is polarized. Polarization is a vector quantity, it has magnitude and direction. These properties are imparted to the piezoceramic during the manufacturing process.

A molecule is polarized if the average position of all of its positive ions is not the same as the average position of all of its negative ions. For example, a water molecule has a bond angle of 104.5° between the oxygen and the two hydrogen atoms. As a result the average position of the two positive ions is not centred on the oxygen ion as it would be if the bond angle were 180° , and therefore the water molecule is strongly polarized.

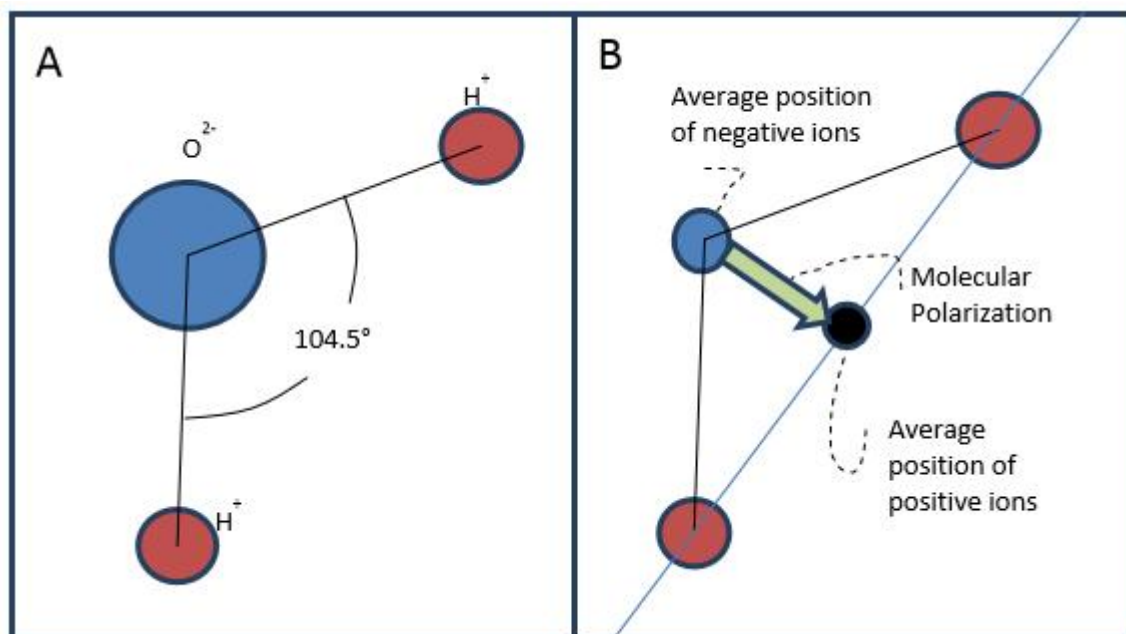


Figure 10 – Polarization in a water molecule [10]

The **Curie temperature** is the critical temperature when the piezoceramics loses its polarization. For example, if the water molecule would be a piezoceramic, then the average bond angle would change to 180° when the temperature exceeds the Curie temperature.

Increasing temperature of the piezomaterial results in a greater internal energy in the material. This causes the negative charged particle to start oscillating from above to below the plane with an average position in the middle of the plane. The crystal structure in a piezoceramic is becoming symmetric above the Curie temperature.

The polarization in a piezoceramic can be explained with a mechanical model of four balls (positive ions) placed in the corners of a square frame. The four balls are connected with springs to a single central ball (negative ion). The bond length (length of the springs) pushes the negative ion out of the plane of the four corner positive ions. The ceramic is now polarized.

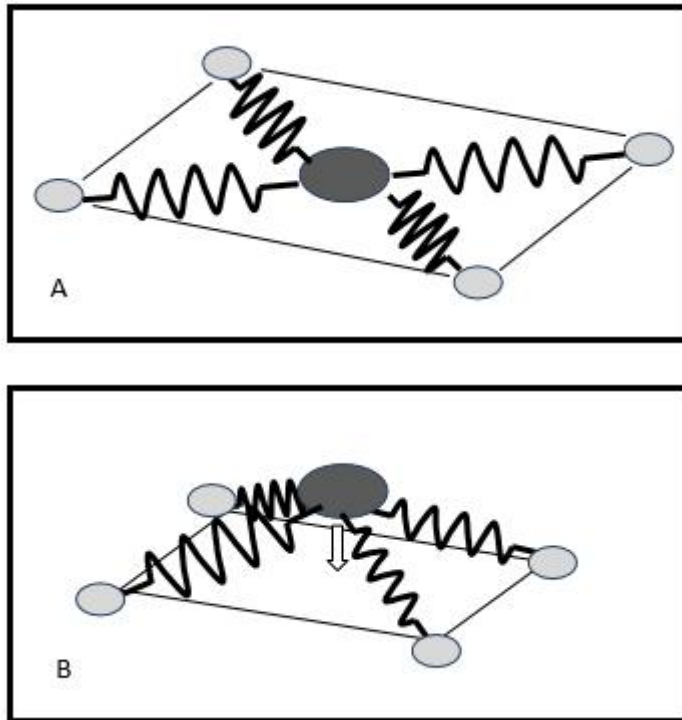


Figure 11 - Polarization in a piezoceramic [10]

Figure 11-A shows a simplified piezocrystal structure above Curie temperature. The negative ion is now oscillating from above to below the plane, and receives an average position in the centre of the plane.

Figure 11-B shows a simplified piezocrystal structure below Curie temperature. The negative ion is now forced to stay either above or below the middle of the plane. The negative ion is now oscillating but with an average position above or under the plane centre position. This is what makes the crystal polarized. The crystal has now received a net polarization in the direction from the negative ion in the direction of the plane (as the arrow describes).

Piezoceramics are not formed by a single crystal, but by grains of crystal separated by glassy interfaces and containing various flaws. These crystals are obtaining a spontaneous

polarization, which means that the direction of the polarization of each crystal differs spontaneously from each other. The net polarization in a sample of a piezoceramic is therefore close to zero. At best the polarization in the sample can be less than 60% of the polarization which could be found in a single crystal of the same formulation.

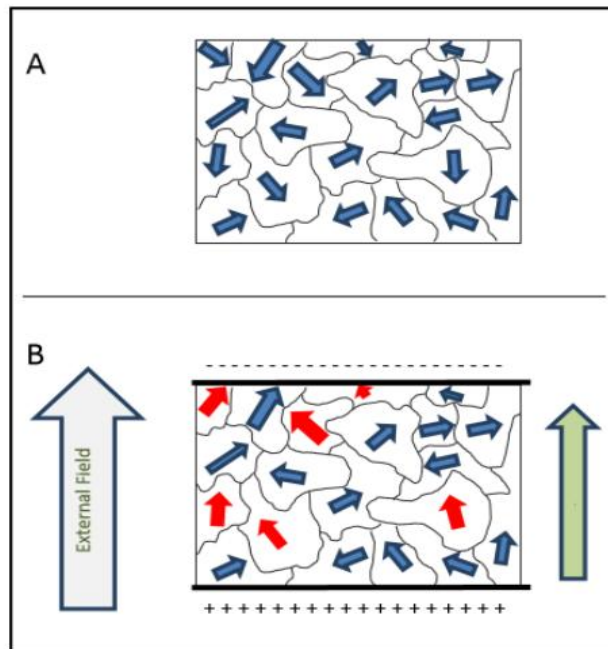


Figure 12 - Polarization in a piezoceramic [10]

Figure 12-A shows a piezoceramic with net polarization zero. This because of the fact that the domains spontaneously points in different directions.

Figure 12-B shows a piezoceramic which is exposed to a large electric field. This field has now flipped direction of some domains so that the net polarization in the material is no longer zero. Note that the majority of the domains now are directed against minus of the electrical field, and only the domains that didn't point that way before changed direction. The same behaviour occurs when an external force is applied on the piezoceramic.

Polarization of a ceramic is not permanent. The polarized ceramic has higher energy and lower entropy than it had before polarization. Random variations due to heat, stress, noise and quantum tunnelling will decrease the polarization of the ceramic. Depoling of a ceramic is usually a logarithmic process. For example, a sample of a piezoceramic may lose 2% of its net polarization in the first hour after being polarized, followed by another 2% the next ten hours, and so on. The rate of depolarization of a piezoceramic increases rapidly as the temperature approaches the Curie temperature of the ceramic. [10]

2.4.4 Mathematical description

This section will present the basic mathematical formulation describing the electromechanical properties of piezoelectric materials. As explained in previous sections, when a polarized piezoelectric material is mechanically strained it becomes electrically polarized, producing a fixed electric charge on the surface of the material. If electrodes are attached to the surfaces of the material, the generated electric charge can be collected and used. Following the linear theory of piezoelectricity, the density of a generated fixed charge in a piezoelectric material is proportional to the external stress. In a first mathematical formulation, this relationship can be simply written as:

$$P_{pe} = d \cdot T$$

Where,

P_{pe} = the piezoelectric polarization vector, whose magnitude is equal to the fixed charge density produced as a result of piezoelectric effect.

d = the piezoelectric strain coefficient.

T = the stress to which piezoelectric material is subjected.

For simplicity, the polarization, stress, and the strain generated by the piezoelectric effect have been specified with the 'pe' subscript, while those externally applied do not have any subscript. In a similar manner, the indirect/reverse piezoelectric effect can be formulated as:

$$S_{pe} = d \cdot E$$

Where,

S_{pe} = the mechanical strain produced by reverse piezoelectric effect

E = the magnitude of the applied electric field.

Considering the elastic properties of the material, the direct and reverse piezoelectric effects can alternatively be formulated as:

$$P_{pe} = d \cdot T = d \cdot c \cdot S = e \cdot S$$

$$T_{pe} = c \cdot S_{pe} = c \cdot d \cdot E = e \cdot E$$

Where,

c = the elastic constant relating the generated stress and the applied strain

$(T=c \cdot S)$, is the compliance coefficient which relates the deformation produced by the application of a stress ($S=s \cdot T$)

e = the piezoelectric stress constant [11]

2.4.5 Usage temperatures of piezoceramic materials

The temperature at which a piezoceramic is to be used is often the most important factor when choosing the piezo material for a specific application. A guideline is to choose the material with the usage temperature not exceeding about half of the Curie temperature of the piezoceramic.

A polarized piezoceramic has decreased entropy. Thermal variations increase the entropy of systems, thus causing parts to depolarize over time. The rate of this depolarization increases over time. The usage temperature is a function of the ambient temperature for the application and the amount of energy that will be dissipated in the ceramic.

For some applications the temperature in the ceramic can be tens or even hundreds of degrees above the ambient temperature. In general, as the temperature rises the useful properties of the piezoceramic will get worse.

Many of the properties of piezoceramics change significantly as the material is heated. For example, the capacitance of piezoceramics rises to a maximum at the Curie temperature, and it can have values which are 50% or higher at its highest working temperature compared to room temperature. [10]

2.5 Pyroelectric effect

Pyroelectric effect is a property of several piezoceramics. The pyroelectric effect is very closely related to the piezoelectric effect. Pyroelectricity (from the Greek pyr, fire, and electricity) is the ability of certain materials to generate a temporary voltage when they are heated or cooled. But when the temperature stabilizes the pyroelectric voltage gradually disappears. All pyroelectric materials are piezoelectric, but not all piezoelectric are pyroelectric.

The change in temperature modifies the crystal structure in such a way that the central negative ion is forced out of its centre position. This is causing a change in the polarization in the same way as when a piezoceramic is exposed to vibration. But in this case the centre negative ion self oscillation increases due to the heat, resulting in a voltage over the crystal. It should be clearly understood that the pyroelectric voltage is not a function of temperature, but only a function of change in temperature. The pyroelectric effect consists of two parts, the primary pyroelectric effect and the secondary pyroelectric effect. The primary effect is the total change in net polarization due to the stress in the ceramic. This is mathematically described as:

$$p = \frac{\partial P_s}{\partial T}$$

The secondary effect is described as the piezoelectric contribution of an electrical voltage due to thermal expansion in the ceramics, mathematically described as follows:

$$p = E \frac{\partial \epsilon}{\partial T}$$

The total mathematical description of the pyroelectric effect is therefore described as:

$$p = \left(\frac{\partial D}{\partial T} \right) = \frac{\partial P_s}{\partial T} + E \frac{\partial \epsilon}{\partial T}$$

Where,

P =Pyroelectrical effect ($\mu\text{As}/(\text{K} \cdot \text{m}^2)$)

D =Electric displacement, charge per unit area (Coloumb/ m^2)

P_s =Polarization

T =Stress (N/m^2)

E =Electric field (Volt/ m)

ϵ =Electrical permittivity

The unit for the pyroelectric effect is usually given as electrical charge / Kelvin · area ($\mu\text{As}/(\text{K} \cdot \text{m}^2)$). [12]

2.6 Knock measurement and sensor failure detection

The knock control application prevents the engine from knocking by controlling the ignition timing (on SG engines) and main fuel injection demand (on SG and DF engines). If cylinder pressure balancing is not available, Knock control application also balances the engine load by controlling main fuel injection between the cylinders when the engine load is high. During normal conditions the air/fuel mixture in the combustion chamber ignites and burns in a controlled manner.

However, during special unwanted conditions, the air/fuel mixture can ignite in an uncontrolled manner creating pressure and temperature peaks in the cylinder which often can be heard as a knocking sound. Knocking can be very damaging for the engine. The engine components cannot withstand severe knocking for any longer periods of time and knocking should hence, when appearing, immediately be neutralized. Figure 13 on the following page describes what knocking looks like. [13]

2.6.1 Knock measurement

Knocking can be measured with two separate sensors, piezo sensors and cylinder pressure sensors. Measurements from these sensors are taken during a specific crank angle window. Once the window has passed, the measurements are analyzed by a DSP (digital signal processor) and the calculated values are provided to the Knock control application. This means that a new knocking value from the piezo sensor and another from the cylinder pressure sensor is available once per engine cycle (720 degrees) for each cylinder. [13]

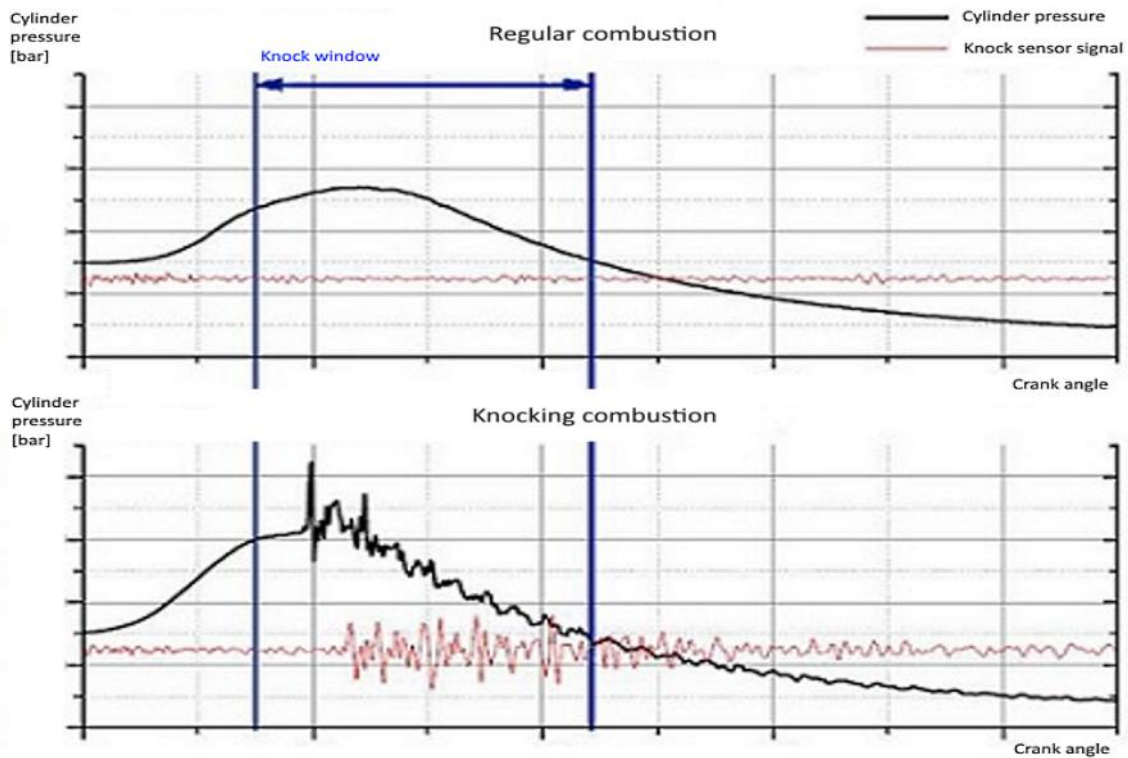


Figure 13 – Knocking [13]

Figure 14 shows example measurement windows of knock from the piezo sensor and knock from the cylinder pressure sensor for a two-cylinder engine. In this example, a total of four knock values are received during one full engine cycle:

1. Knocking value from the piezo sensor of cylinder A1
2. Knocking value from the cylinder pressure sensor of cylinder A1
3. Knocking value from the piezo sensor of cylinder A2
4. Knocking value from the cylinder pressure sensor of cylinder A2

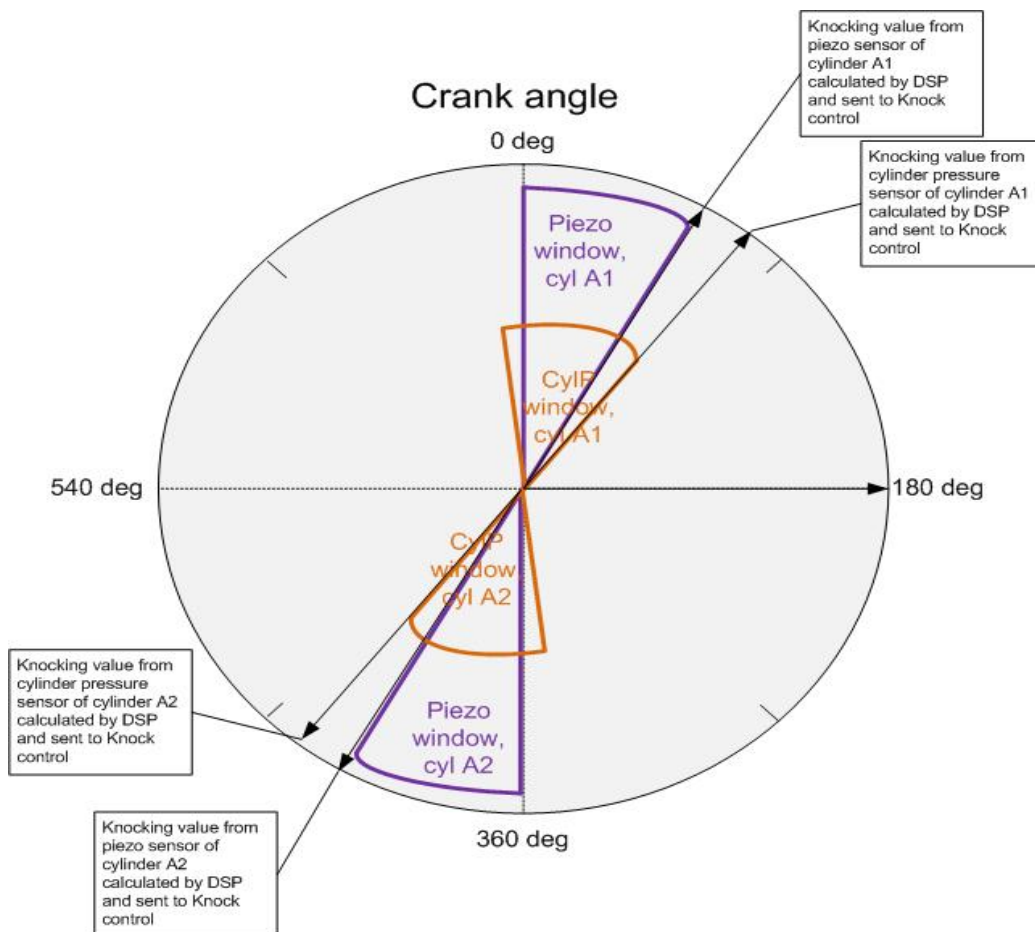


Figure 14 –Measurement windows [13]

The knock control function prevents the engine from knocking by controlling the ignition timing (on SG engines) and main fuel injection demand (on SG and DF engines). The control of the ignition and fuel demand is done in a cylinder wise manner. The knock control function can also, if necessary, automatically initiate a gas trip, load reduction or shutdown of the engine.

2.6.2 Sensor failure detection

The cylinder pressure and piezo sensors are connected to the DSP on the CCM. A DSP calculates separate piezo and cylinder pressure knock values from the raw signals and sends them as knock sample messages to the Knock control application. Each sample holds the latest raw knock value and the sensor failure status. The piezo sensor signal is used only for knock detection but the bell shaped cylinder pressure signal is also used for detecting other pressure related values (e.g. cylinder peak pressure). The piezo knock sensor is stated faulty, when a sample sent by the CCM module has the sensor failure status active. [13]

To be able to detect a sensor failure, when using charge type knock sensors (piezo electric sensors), a so-called “DC-method” is used. The DC-method works in the following way:

The sensor signal is biased, by connecting the sensor output in such a way, that it constitutes a loop with a DC-source. This source is part of the cylinder controller electronics, and will work as a voltage divider together with the internal resistance of the sensor. The DC-source biases the signal from the knock sensor, as long as the signal loop is healthy.

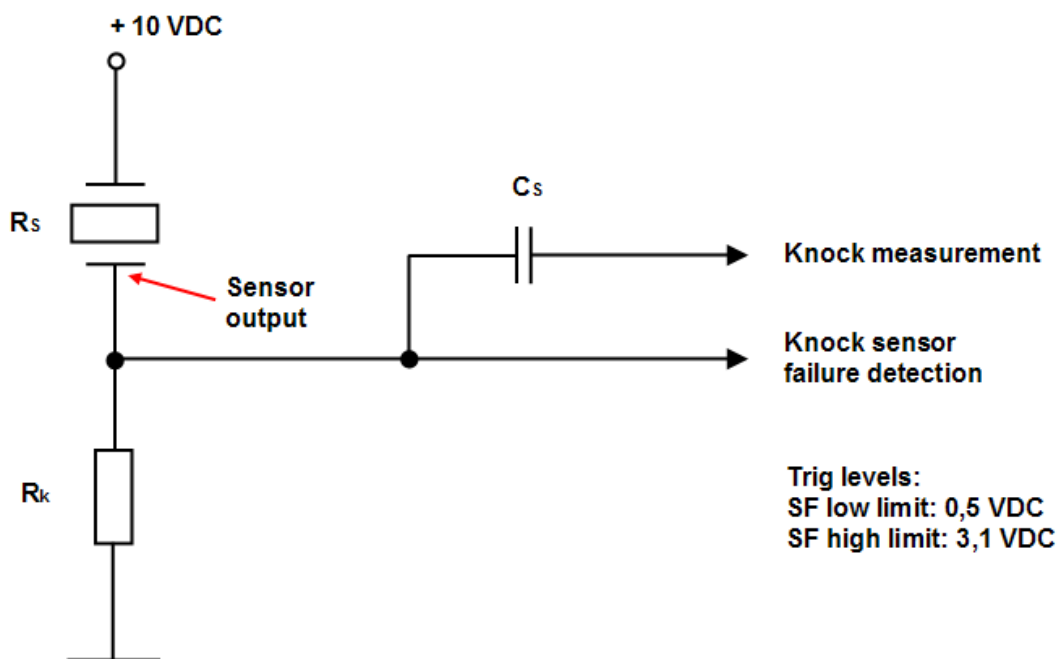


Figure 15 - DC method [14]

For knock detection a high-pass filter is used, because only the AC-component contains knock information. Before a location in the signal treatment, where this high-pass filtering occurs, the detection of sensor failure is provided. At this point a voltage measurement is provided. A cable break or a break inside the sensor itself will disconnect (open) the DC-loop, thus create a DC-voltage which is less than 0.5 V. A short circuit in the sensor or in the sensor cable, will create a DC-voltage which is higher than 3.1 V. Both these thresholds are monitored in the cylinder controller electronics. The SF alarm for the specific cylinder will activate, if the DC-level goes beyond one of these pre-defined levels. [14]

2.6.2.1 Knock sensor replacement circuit

A replacement circuit for a knock sensor and a model for the whole knock sensor diagnostic circuit were built to be able to simulate the system. This can later be used to verify how the knock sensor diagnostic system responds to different insulation resistances. The replacement circuit for a knock sensor is shown below in figure 16. It can be described as a circuit with the following components:

- Shunt resistor – The resistance of the insulation discs
- AC voltage source – Charge powered by acceleration/vibration
- Capacitor – Piezoceramic capacitance
- Insulation resistance resistors – corresponds the pin to support sleeve resistances.

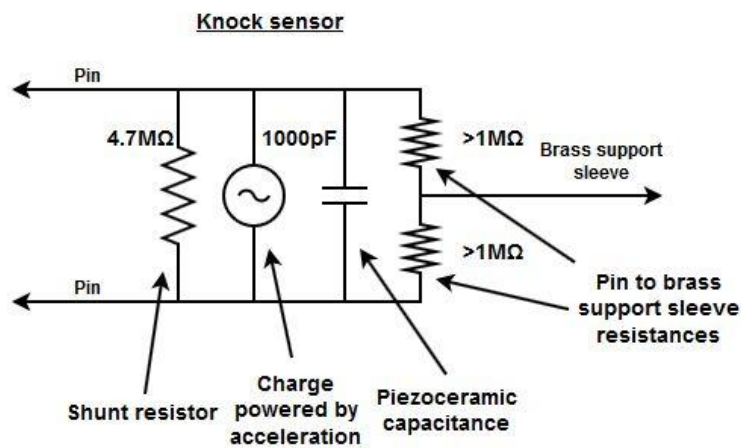


Figure 16 - Knock sensor replacement circuit

2.6.2.2 Sensor failure diagnostic circuit

2.7 Root Cause Analysis theory

“A Root Cause is the cause where a solution is implemented to solve the problem” [Mark Wildi, Root Cause analysis course. 24.11.2014]. Root Cause analysis (RCA) is a method of problem solving that tries to identify the root causes of faults or problems. A Root Cause is a cause that once removed from the problem fault sequence, prevents the final undesirable event from recurring. A condition is a factor that affects an action's outcome. Removing a condition can benefit an outcome, but it does not necessarily prevent its recurrence. [15]

2.7.1 Realitycharting process

Realitycharting is the name of the Root Cause analysis method which is used in this thesis. This method is most easily understood by looking at an example of a simple problem. Let's say that a fire has started on a chair in your apartment, and now you want to use the realitycharting method to find out the Root Cause (why the fire started). A candle was placed on the chair when the fire started.

This is the realitycharting process:

1. Define the problem

- Write down the following
 - What – The primary effect
 - When
 - Where
 - Significance- Why you want to prevent it

So, for the fire on the chair it could look like this:

What:	Fire
When:	1.1.2015
Where:	In my apartment
Significance:	Damaged chair

Figure 17 - Problem definition

2. Create a Realitychart

- For each effect ask “why”?
- Look for causes in Actions and Conditions
- Connect causes with “Caused by”
- Support causes with evidence or use a “?”
- End with stop or “?”

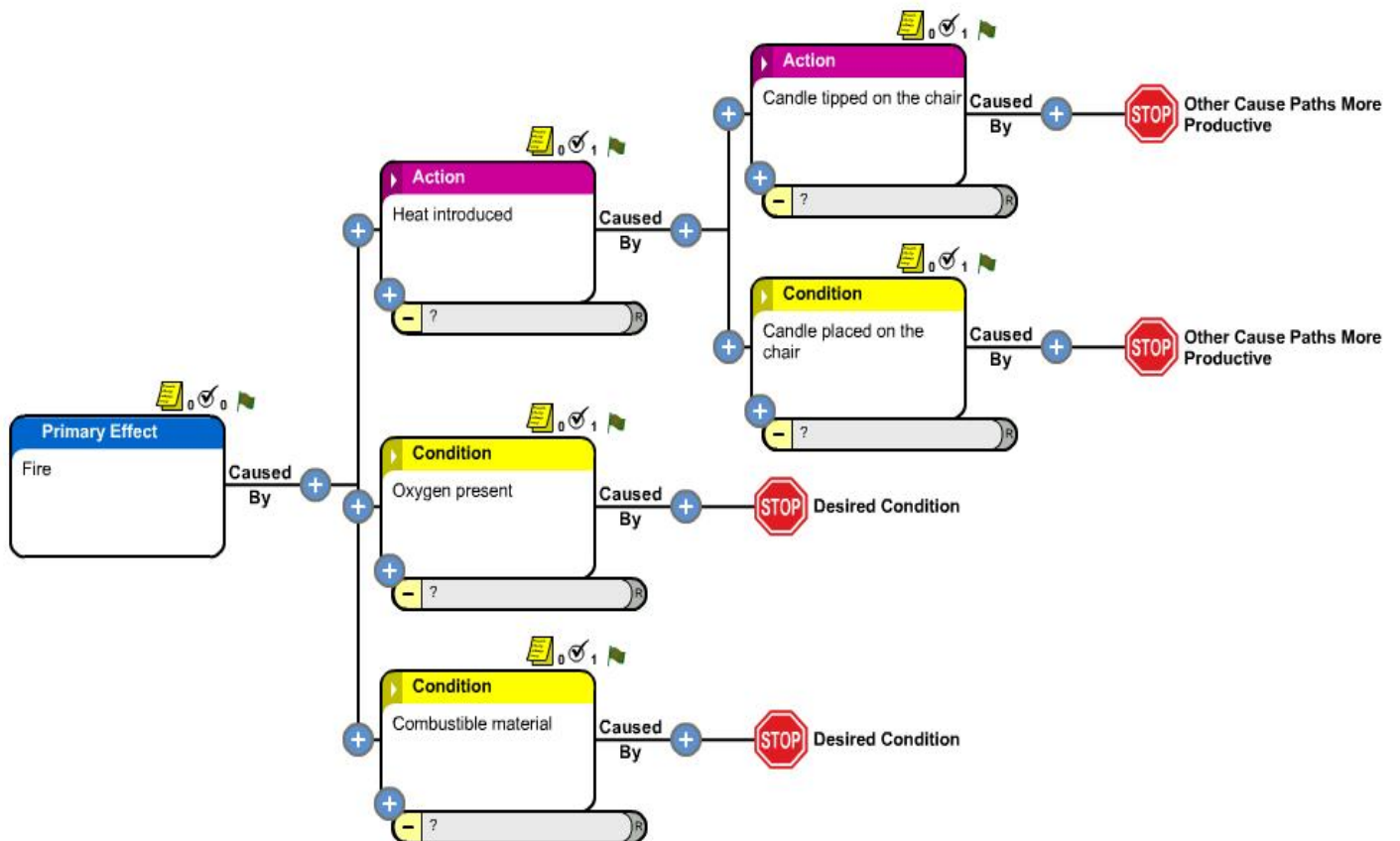


Figure 18 - Realitychart

When going from right to left in the chart you go in the direction of time, i.e. first the candle tipped on the chair which introduced heat to the chair and finally the fire started. The direction from left to right, when looking at the chart, is called *direction of causation*. This means that the fire was caused by the introduced heat which in its turn was caused by the fact that the candle tipped on the chair.

3. Identify effective solutions

- Look for solutions that remove, change, or control a cause
- Identify the best solutions – they must:
 - Prevent recurrence
 - Be within your control
 - Meet your goals and objectives
 - Not cause other problems

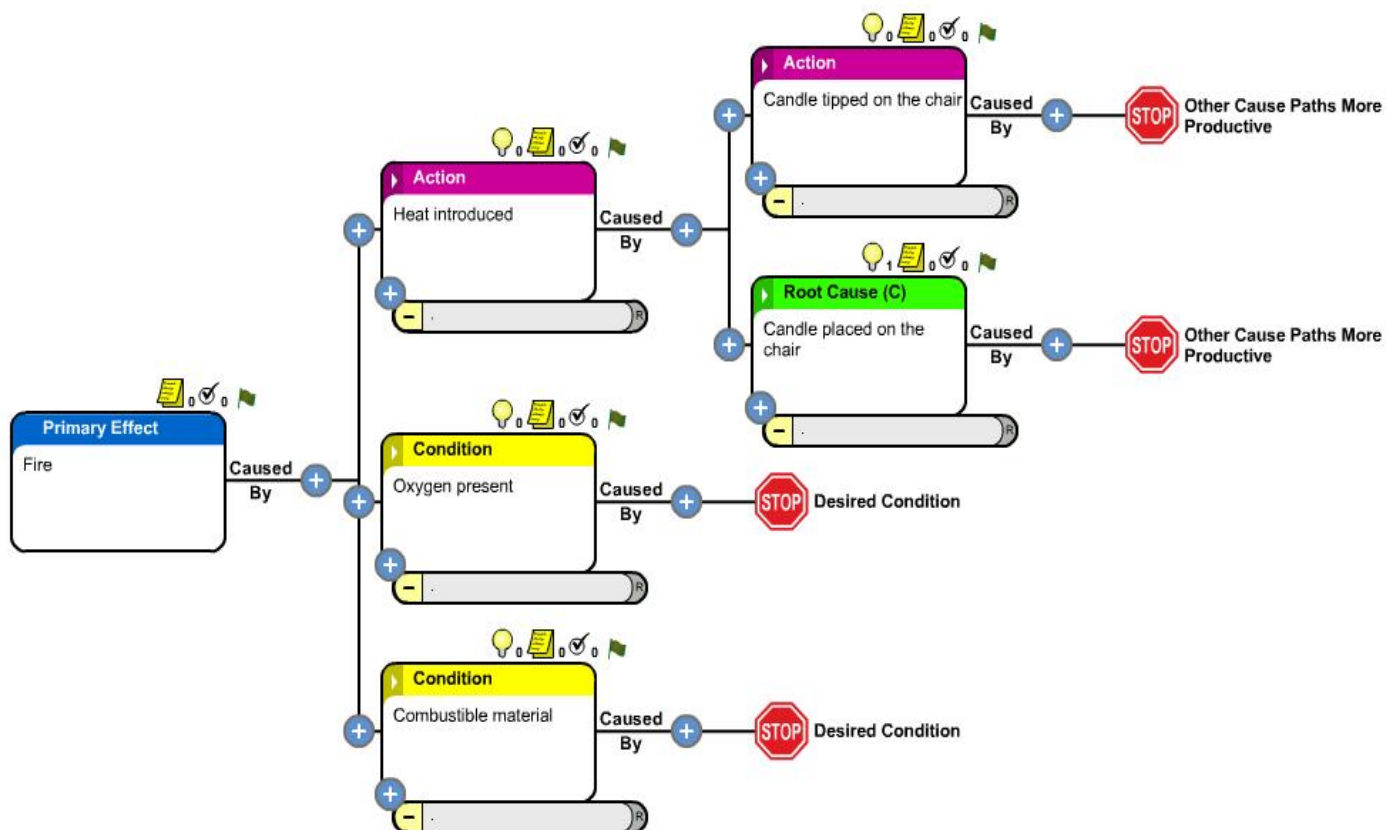


Figure 19 – Reality chart with an implemented solution

When implementing the solution “*Do not place a candle on the chair*” on the “*candle placed on the chair*” condition, the program automatically marks the condition as a root cause (the solution cannot be seen in the chart). [16]

3 Tests

In this chapter all performed tests have been documented. Both KS1 and KS4 sensors have been tested in a, for the purpose, specially built test cabinet. The tests have been performed with both heat and vibration as affecting variables. A sensor named the “good” sensor is an old working sensor, which is used as reference in several tests.

3.1 General information

The investigations of the knock sensors were, for a long time in the beginning of the tests, focused on the pyro-electric effect, but this is not the phenomenon that causes the fluctuations of the diagnostic values.

The insulation resistance measurements on knock-sensors, which are documented in a forthcoming chapter, have shown that the main reason for the changing diagnostic values is poor insulation resistances. When the sensors warm up (80-100 °C) the insulation resistance drops remarkably, which in its turn causes the knock sensor diagnostic values to drop/rise depending on the engine block potential. The poor insulation resistance is in its turn caused by moisture in the sensor moulding material.

Samples of a new model of the Bosch knock sensor, the KS4 model, were ordered and to be tested and compared with the KS1 model. If the KS4 sensor is suitable for the knock system and shows better results than the KS1 sensor, changing to the KS4 sensor as standard on gas engines will be the optimal solution.

3.2 The initial problem

The initial problem concerning knock sensor diagnostic value fluctuations occurred at vessels with 50DF engines equipped with WECS 8000 and KSFD card. When replacing old KS1 sensors with new KS1 sensors on engines, the diagnostic values drop/rise causing sensor failure alarm.

At a customer ship the sensor change from old KS1 sensors to new ones resulted in a majority of the diagnostic values dropping below the knock sensor failure low limit. Originally the knock sensor failure limits are set at 500 mV and 3100 mV. Figure 21 shows the knock values on an engine after all knock sensors had been replaced with new KS1 sensors. As seen in figure 21, 11 out of 12 sensors are below the low limit (500 mV) after changing to new KS1 sensors.

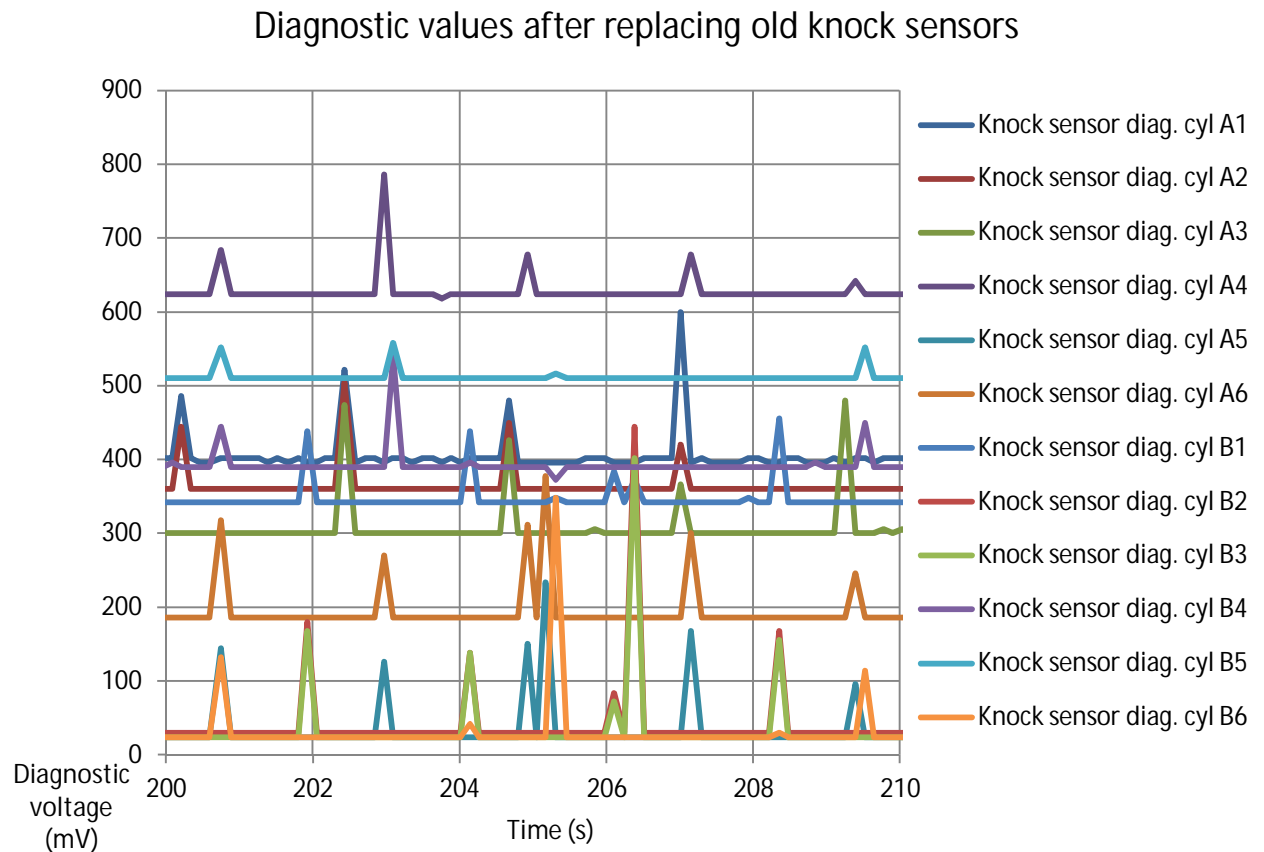


Figure 20-Diagnostic values at a customer ship after changing to new KS1 sensors

3.3 Heat cabinet

Before the testing could start a heat/vibration test bench had to be built. The test bench was made from three basic parts, a vibration bench, an electric cabinet and a hotplate. The cabinet was mounted on top of the vibration bench with four threaded rods. The hot plate was mounted inside the cabinet next to a fan which circulates the air in the cabinet. A thermostat regulates the temperature in the cabinet.



Figure 22 - Heat cabinet



Figure 21- Knock sensors mounted in the heat /vibration cabinet

Figure 23 shows what the complete heat/vibration bench looks like. Figure 22 shows three knock sensors mounted on the vibration bench. The temperature sensor in the middle measures knock sensor temperature. A temperature sensor beside the vibration head measures the air temperature inside the cabinet. A regular frequency generator was used to generate the desired frequencies for the vibration exciter.

3.4 KS1 heat test with WECS 8000

15 knock sensors were received from a customer ship. The sensors were said to be defect and will now be tested by heating them up to 120 degrees Celsius and at the same time logging the output with Wecsplorer. The "good" sensor is also tested and plotted in the same graph as the other sensors. The sensors are tested three at a time in a WECS 8000 test rig.

3.4.1 Test results

During the test procedure all sensors were heated up to 120 °C in the heat/vibration cabinet until the diagnostic signal stops rising. The results have been summarized in Figure 25. The graph shows all sensors that have been tested and also the "Good" sensor is included.

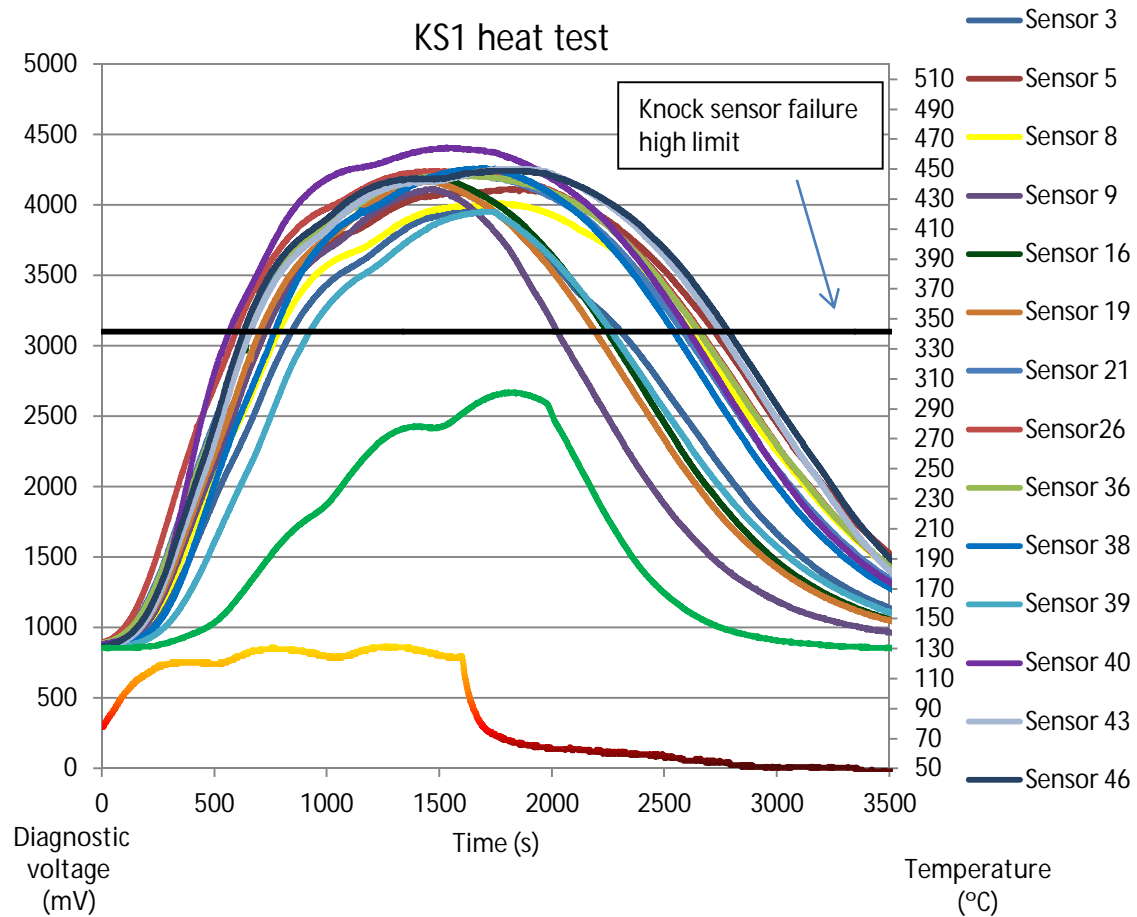


Figure 25 - KS1 heat test

As can be seen in figure 25 all KS1 sensors are exceeding the knock sensor failure limit with over 1000 mV at 125 °C, while the "Good" sensor maximum diagnostic voltage output is 2700 mV. It can also be noted that all sensors from the ship have the same characteristics, which means that the high diagnostic voltage output can be a result from the manufacturing of the sensors.

3.5 KS1 drying test

When this test was planned the intentions were to investigate if it was poor aged piezo material in the sensors that could be the reason for the rising diagnostic voltage. When the insulation resistance tests in *chapter 3.6* were performed it was clear that this was not the case.

The "aging" process is a part in the manufacturing of the piezo knock sensors when the piezo-discs for a period are exposed to high temperature in order to make the sensors

stable. The aging process at Bosch's factory is performed by heating up the piezoelements to 240 °C for 5 hours in an oven.

When trying to heat up a complete knock sensor to 240 °C it was noticed that the molding material on the sensor becomes too soft and the sensor begins to lose its shape. Therefore the temperature was decreased to 210 °C when aging them. Sensors no 3, 5 and 8 were heated up to 210 °C for 6 hours to see if the pyro-electric voltage is remarkably affected by the aging process. After the heating the aged sensors were tested again in the oven at 120 °C and the outputs from the sensors were logged with wecsplorer.

The diagnostic output characteristics of the sensors before aging and after aging are both compared in figure 26.

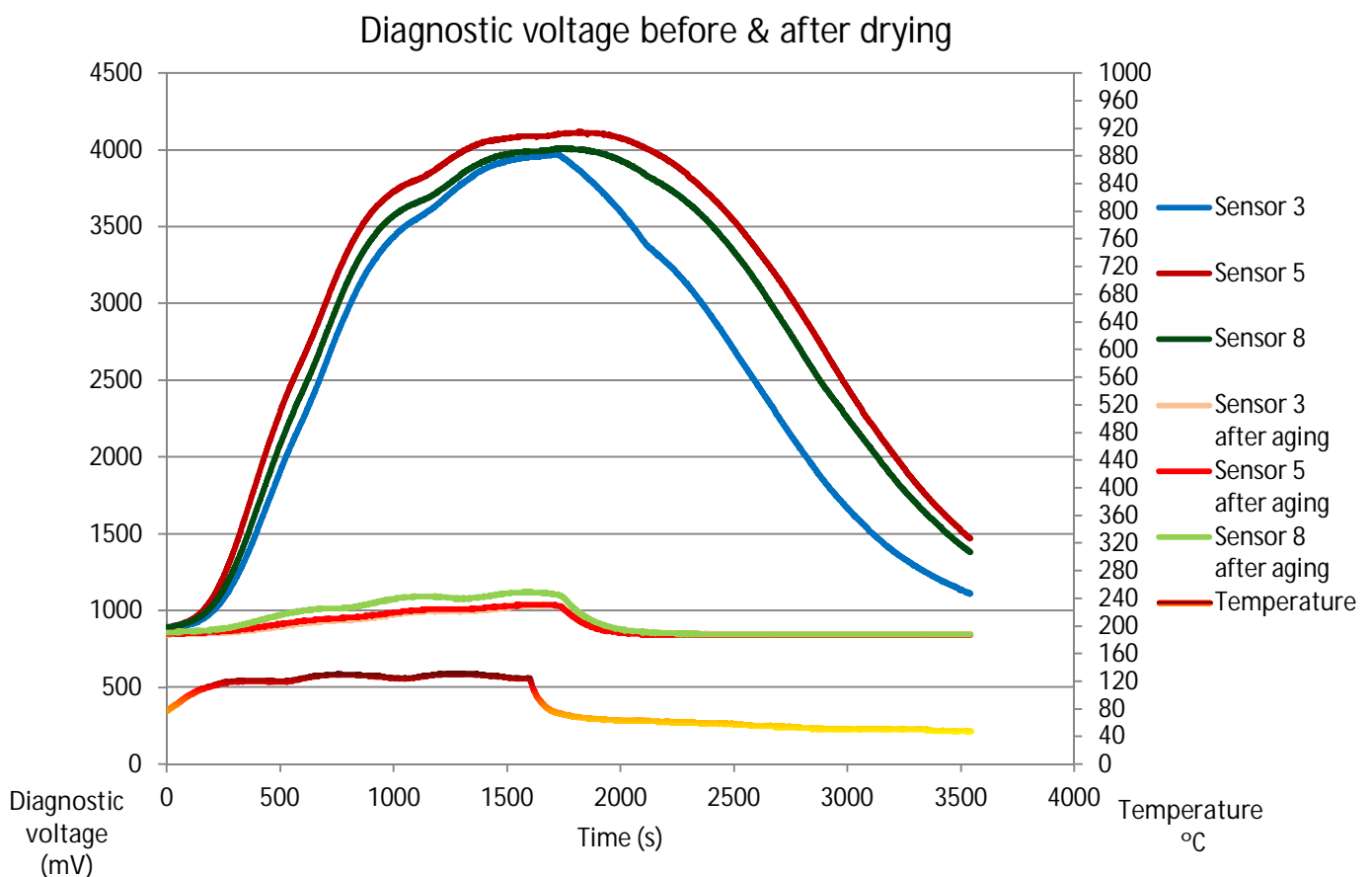


Figure 26 - Diagnostic voltage comparison

As can be seen in the diagram the diagnostic voltage has decreased remarkably after aging the sensors. The highest diagnostic voltage observed after drying at the same temperature (120 °C) is 1100 mV, about 3000 mV lower than before the drying procedure.

3.5.1 Different drying times

As the sensors could not stand heat up to 240 °C a new test was performed but now at a temperature of 150 °C. The tested sensors are number 9, 16 and 19. The drying times will be 2.5 h for sensor no 9, 5 h for sensor no 16 and 7.5 h for sensor no 19.

The results are compared in figure 27.

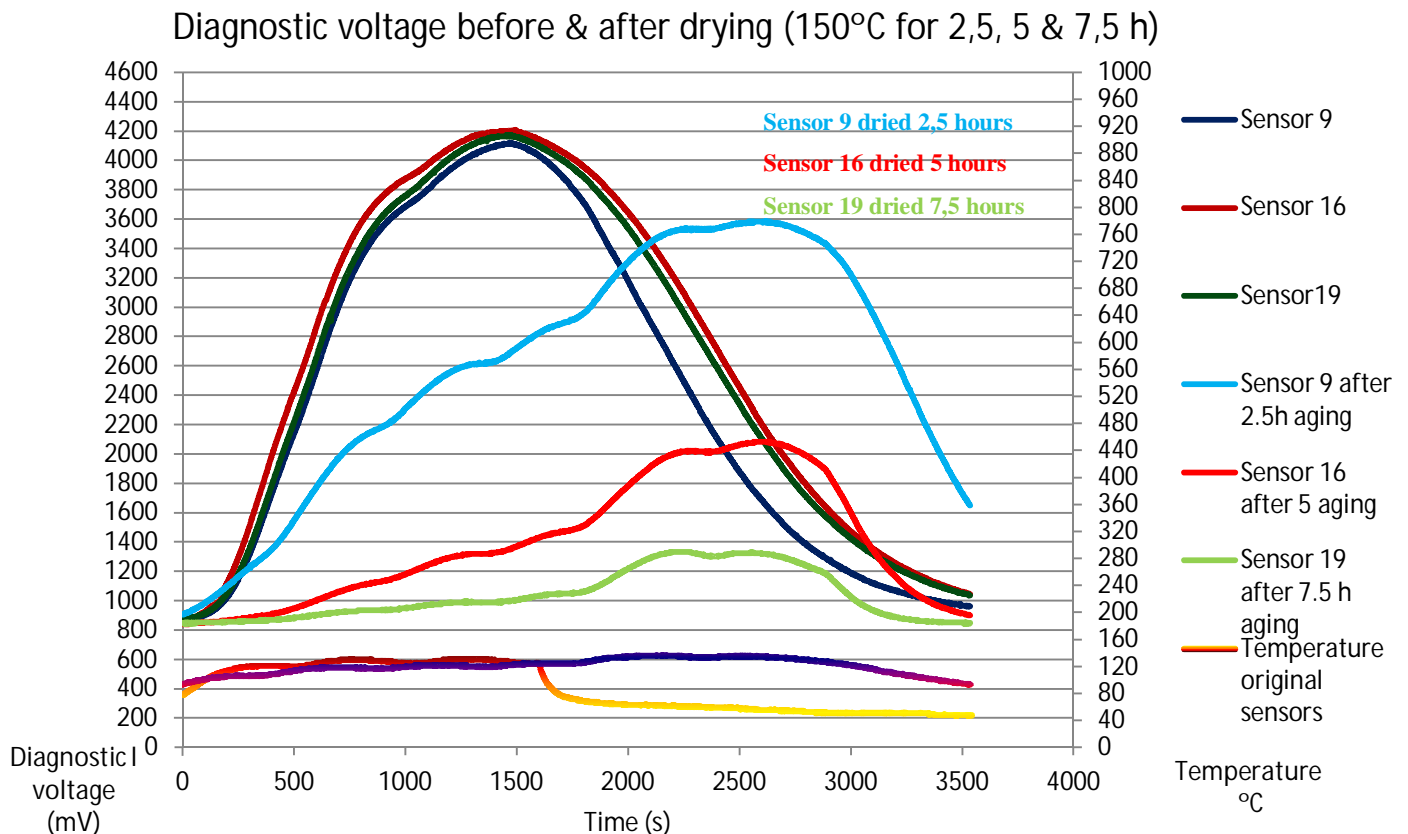


Figure 27 - Diagnostic voltage comparison

As can be seen in the diagram the diagnostic voltage decreases remarkably when extending the aging time. After 2,5 hours the diagnostic voltage has dropped with about 500 mV, after 5 hours it has decreased to half of its original value and after 7,5 hours it has decreased with about 2900 mV.

It can also be noticed that the diagnostic voltage rises more slowly for the aged sensors than for the unaged sensors when exposing them to a high temperature.

3.5.2 Drying time

Figure 28 shows how the drying time affects the diagnostic voltage at a temperature of 150 °C. This diagram is based on the results from the test when sensors 9, 16 and 19 were dried.

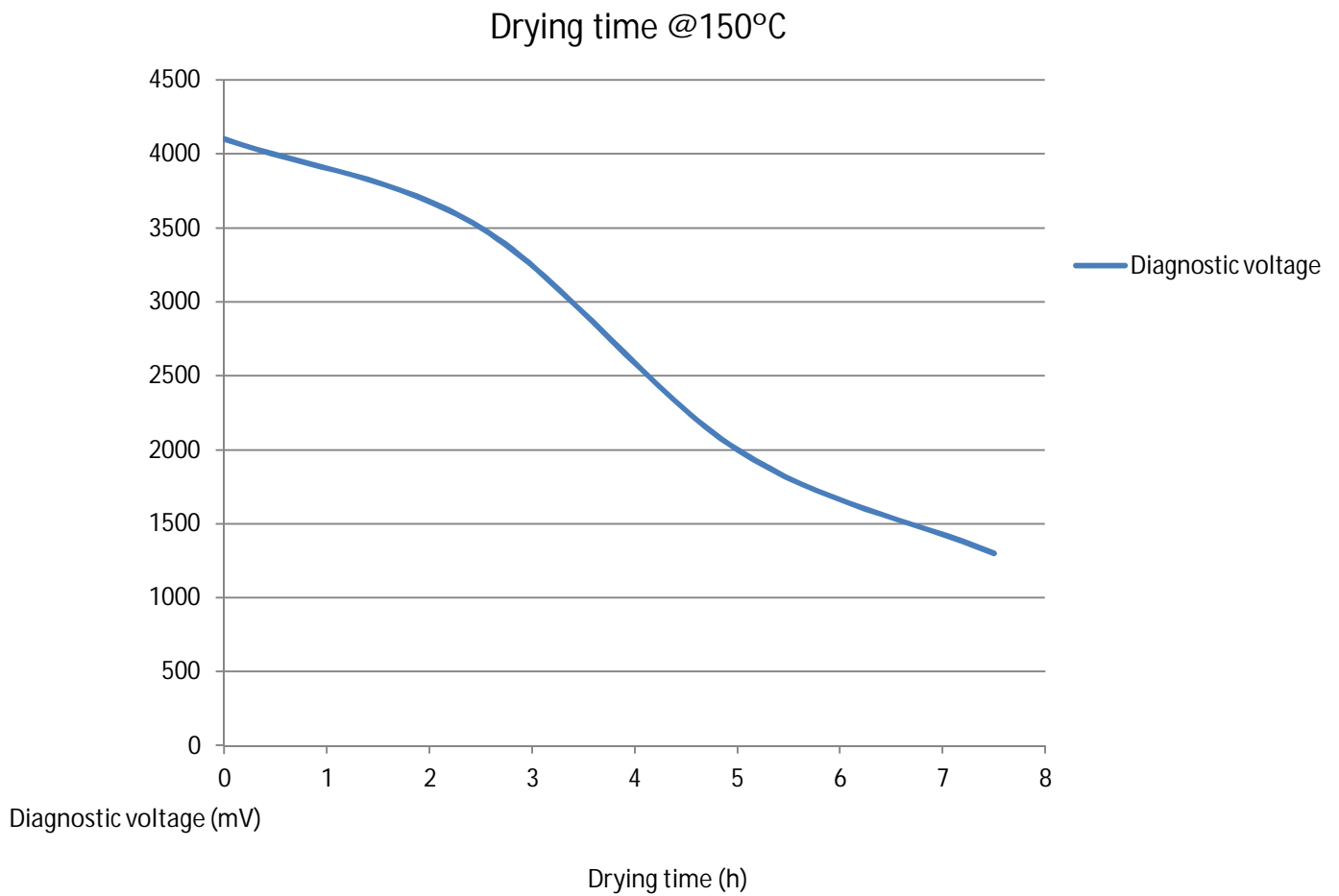


Figure 28 - Drying time for KS1 sensors

3.5.3 Temperature test 2 weeks after drying

Sensors 3, 5, 8 and 9, 16, 19 were tested again in the same way as they were tested two weeks after they had been dried.

Sensor 9, 16, 19

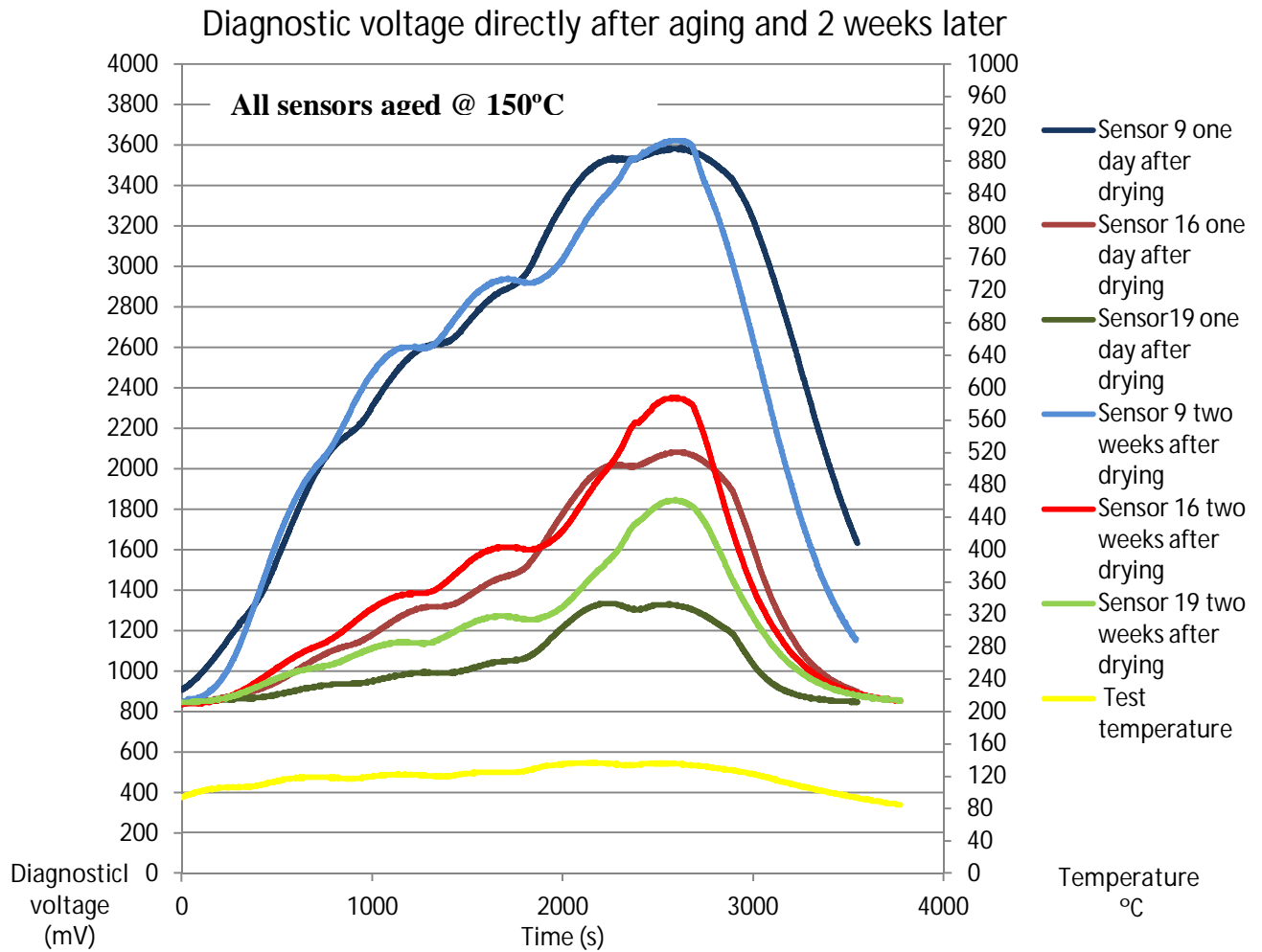


Figure 29 - Diagnostic voltage comparison

As can be seen sensor 9 has not changed remarkably but sensor 16 has got a higher diagnostic output. Sensor 19 has worsened most, approximately twice as much as sensor 16. It can be seen from these results that the sensors are, after drying, creeping back to a larger diagnostic voltage output. If the sensors have been dried for a longer time, they return faster to a larger diagnostic output than the sensors that have not been dried for an equally long time.

Sensors 3,5,8

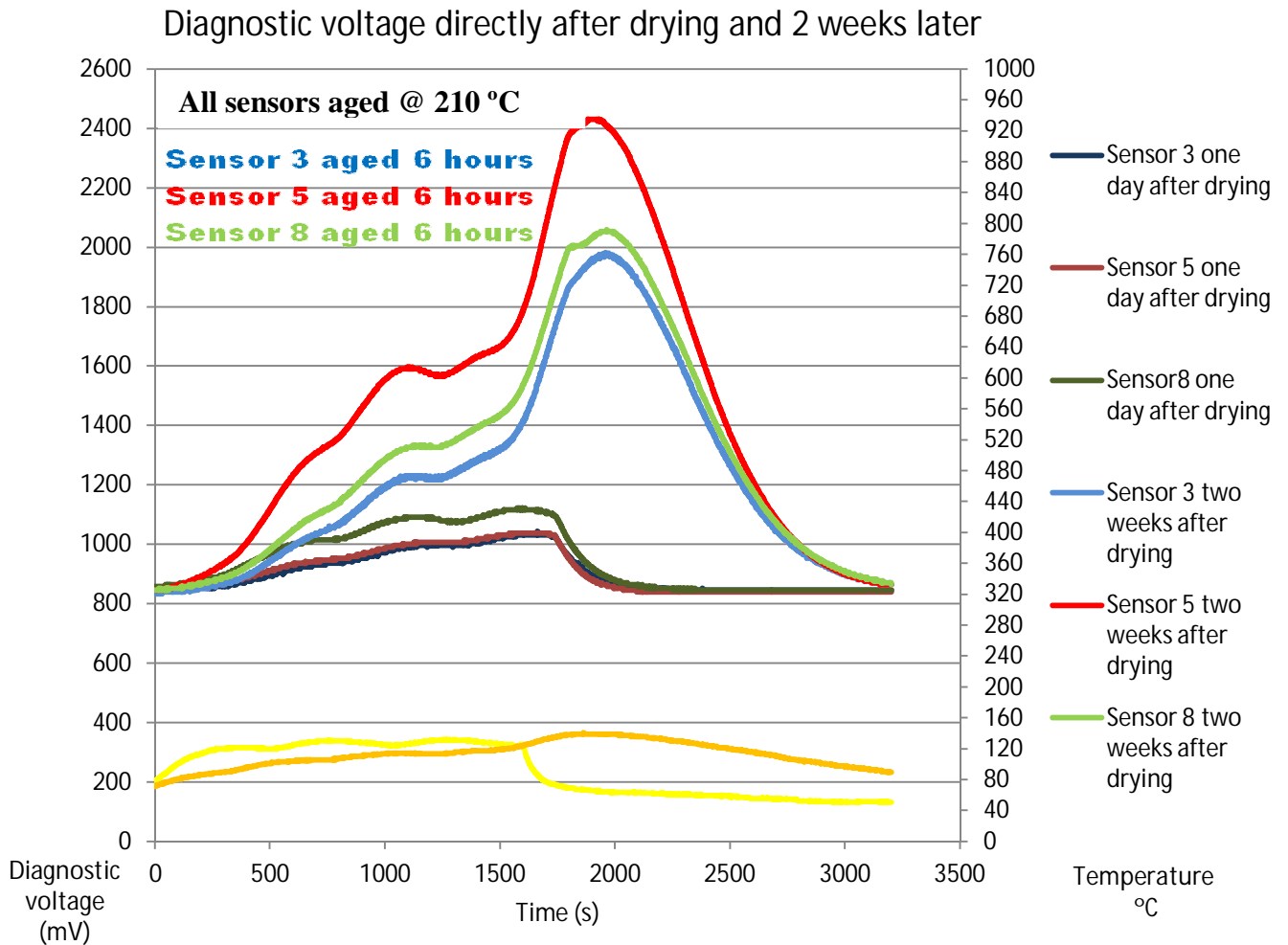


Figure 30 - Diagnostic voltage comparison

After two weeks the diagnostic voltage for sensors 3, 5 and 8 has risen remarkably. All these sensors were aged at the same temperature (210 °C), and for an equally long period (6h). Note that the testing temperature went approximately 10 °C higher in the newer test and may have caused a bit too high results compared to the previous test, but still it can be stated that the diagnostic voltage output increases by time after drying, when sensors are stored at room temperature.

3.5.4 Mounting torque test

In this test sensors no 21, 26 and 36 were tested with different mounting torques to see if it affects the diagnostic voltage output from the sensor. The sensors were mounted on different iron plates to avoid appearance of interference between them. On an engine the mounting torque is 20 Nm for the knock sensors. The different torques that will be tested are therefore 20, 35 and 50 Nm. The test was performed in the same way as previous tests, i.e. by heating up the sensors to 120 °C and at the same time logging the results with Wecsplorer.

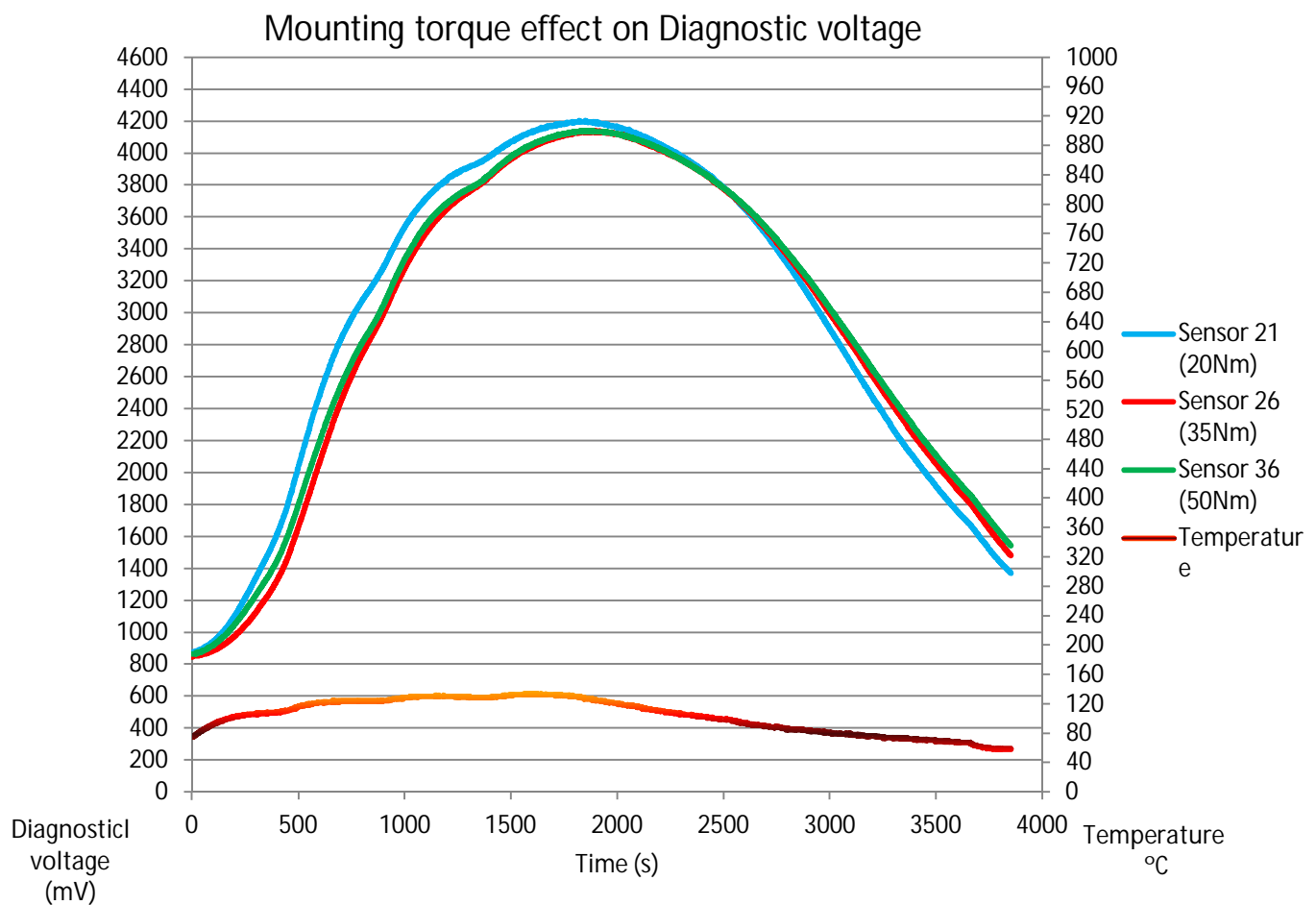


Figure 31 - Mounting torque test

As can be seen in this graph the mounting torque does not affect the diagnostic voltage at all. The same voltage levels are reached independently of the mounting torque.

3.5.5 Pyro-electric effect proof

The pyro-electrical effect, which was the main suspect for this problem for a long time is confirmed not to be affecting the diagnostic system remarkably. Pyro-electrical voltage can only be produced by a piezoceramic when the material is heated up or cooled down. At a stable temperature there is no pyro-electrical voltage produced by the sensors.

The knock sensors produce a maximum pyro-electrical voltage of about 50-70 mV. Figure 32 shows a voltage output from a KS1 sensor when it is first cooled down to approximately -15 °C and then heated up to +60 °C.

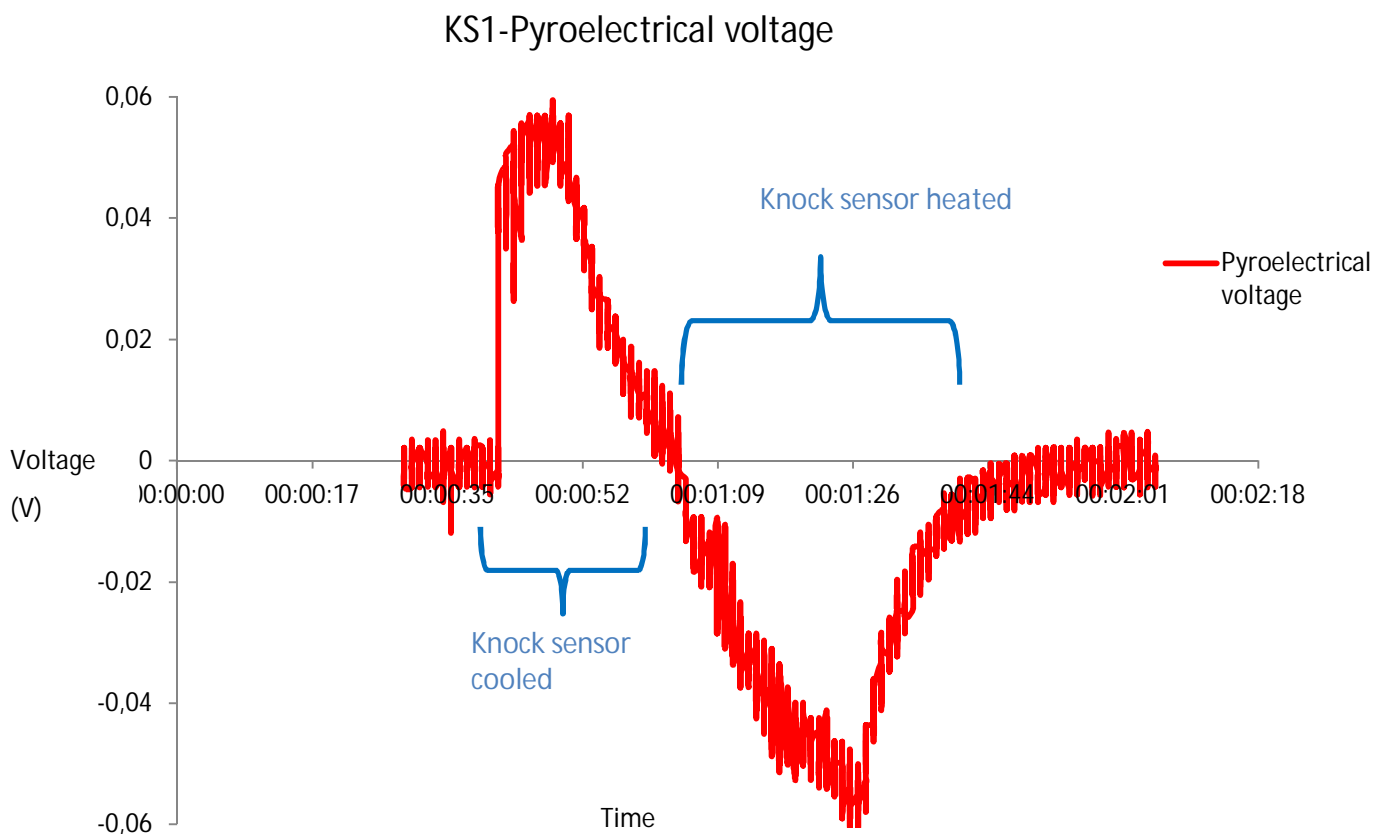


Figure 32 - Pyroelectric voltage generated by temperature changes

If this test was performed with inverse polarity, the pyro-electrical voltage output would also be inverted compared to this result. Further cooling or heating would not result in a higher pyro-electrical voltage. Due to the fact that the pyro-electrical voltage levels are this low the **effects on the diagnostic system will be insignificant.**

3.6 Insulation resistance test

The main cause of the rising/dropping diagnostic values is concluded to be the poor insulation resistance that some batches of the new KS1 sensors have demonstrated. The insulation resistance is specified to $>1 \text{ M}\Omega$ for both KS1 and KS4 sensors. The operating temperature range is -40 to $150 \text{ }^\circ\text{C}$. But when sensors are heated, the insulation resistance drops remarkably, and already at a temperature of $95 \text{ }^\circ\text{C}$ some sensor batches show values around $500 \text{ k}\Omega$.

Table 1 contains test results from the insulation resistance measurements performed on the knock sensors. The resistance between each pin and ground and the resistance between the two pins have been tested. These tests have been performed at both $20 \text{ }^\circ\text{C}$ and $95 \text{ }^\circ\text{C}$. The resistance in the $20 \text{ }^\circ\text{C}$ tests is given in $\text{G}\Omega$, while the resistance in the $95 \text{ }^\circ\text{C}$ tests is given in $\text{M}\Omega$ or $\text{k}\Omega$.

The measurements were performed with the Megger MIT1020/2 insulation tester. All measuring was performed at 100 V , and at the temperatures $20 \text{ }^\circ\text{C}$ and at $95 \text{ }^\circ\text{C}$. Results for KS1 and KS4 sensors are given in separate tables.

3.6.1 Test results

KS1 test results

Table 1- Results from KS1 sensor insulation tests

Model	y/m	Right pin to support sleeve $20 \text{ }^\circ\text{C}$ ($\text{G}\Omega$)	Right pin to support sleeve $95 \text{ }^\circ\text{C}$ (Ω)	Left pin to support sleeve $20 \text{ }^\circ\text{C}$ ($\text{G}\Omega$)	Left pin to support sleeve $95 \text{ }^\circ\text{C}$ (Ω)	Pin to Pin $20 \text{ }^\circ\text{C}$ (Ω)	Pin to Pin $95 \text{ }^\circ\text{C}$ (Ω)
KS1	04/4	250	4M	200	2M	4,7M	2M
	05/11	270	3M	>300	2M	4,7M	1.8M
	09/8	230	3M	260	2M	4,7M	1.6M
	05/11	>300	3M	290	2M	4,7M	2M
	11/5	11	790k	11	390k	4,7M	530k
	11/5	9	430k	9	570k	4,7M	640k
	11/5	8	390k	8	520k	4,7M	800k
	11/5	7	380k	7	270k	4,7M	540k
	11/5	7	350k	7	250k	4,7M	600k
	11/5	9	310k	10	350k	4,7M	800k
	11/5	7	700k	8	500k	4,7M	870k
	11/5	7	500k	7	500k	4,7M	950k

As can be seen when comparing the KS1 sensors, the insulation resistance for the 11/5 dated sensors is much lower than for the other KS1 batches.

KS4 test results

Table 2 - Results from KS4 sensor insulation tests

Model	y/m/d	Right pin to support sleeve 20 °C (GΩ)	Right pin to support sleeve 95 °C (Ω)	Left pin to support sleeve 20 °C (GΩ)	Left pin to support sleeve 95 °C (Ω)	Pin to Pin 20 °C (Ω)	Pin to Pin 95 °C (Ω)
KS4	14-10-02	>300	6M	>300	2M	4,7M	3.5M
	14-06-30	290	3.5M	>300	4M	4,7M	3M
	14-10-02	>300	8M	>300	4M	4,7M	4M
	14-10-02	>300	8M	>300	5M	4,7M	4M
	14-10-02	>300	8M	>300	7M	4,7M	4M
	14-10-02	>300	8M	>300	6M	4,7M	4M
	14-10-02	>300	4M	>300	3M	4,7M	2M
	14-10-02	>300	4M	>300	3M	4,7M	2M
	14-10-02	>300	4M	>300	3M	4,7M	2M
	14-06-30	>300	1.8M	>300	1.4M	4,7M	1M
	14-06-30	>300	1.5M	>300	1.6M	4,7M	900k
	14-06-30	>300	1.6M	>300	1.7M	4,7M	1M

When comparing the KS4 sensors we can see that the 14-10-02 dated batch is better than any of the KS1 sensor batches, but the insulation resistance for the 14-06-30 batch is sometimes lower than for some of the KS1 batches.

The sensors with the lowest insulation resistance show a resistance (pin to support sleeve)

KS4 with new molding material test results

Table 3 - Results from KS4 sensor with new molding material insulation tests

Model	y/m/d	Right pin to support sleeve 20 °C (GΩ)	Right pin to support sleeve 95 °C (Ω)	Left pin to support sleeve 20 °C (GΩ)	Left pin to support sleeve 95 °C (Ω)	Pin to Pin 20 °C (Ω)	Pin to Pin 95 °C (Ω)
KS4	15-01-28	>300	76M	>300	83M	4,7M	4,7M
	15-01-26	>300	77M	>300	83M	4,7M	4,7M
	15-01-26	>300	88M	>300	90M	4,7M	4,6M
	15-01-26	>300	90M	>300	104M	4,7M	4,6M
	15-01-26	>300	130M	>300	135M	4,7M	4,7M

of $>70 \text{ M}\Omega$ at $95 \text{ }^\circ\text{C}$. This is remarkably higher compared to previous tests with sensors with the old molding material. It can also be noted that pin to pin resistance does not change from the specified $4.7 \text{ M}\Omega$. Using this sensor model would therefore be a good solution for the problem seen from the sensor failure detection aspect.

Figure 33 shows a KS1 and a KS4 sensor that have been trended in parallel when the temperature was increased from $20 \text{ }^\circ\text{C}$ to $95 \text{ }^\circ\text{C}$. The test time is 25 minutes (1500 seconds). The KS1 sensor is from batch 11/5 and the KS4 from batch 14-10-02. The resistance is measured from the right pin to the Brass support sleeve. Note that the resistance is in a logarithmic scale in the diagram. After the previous test was done we received a KS4 model with the new kind of molding material which was tested in the same way.

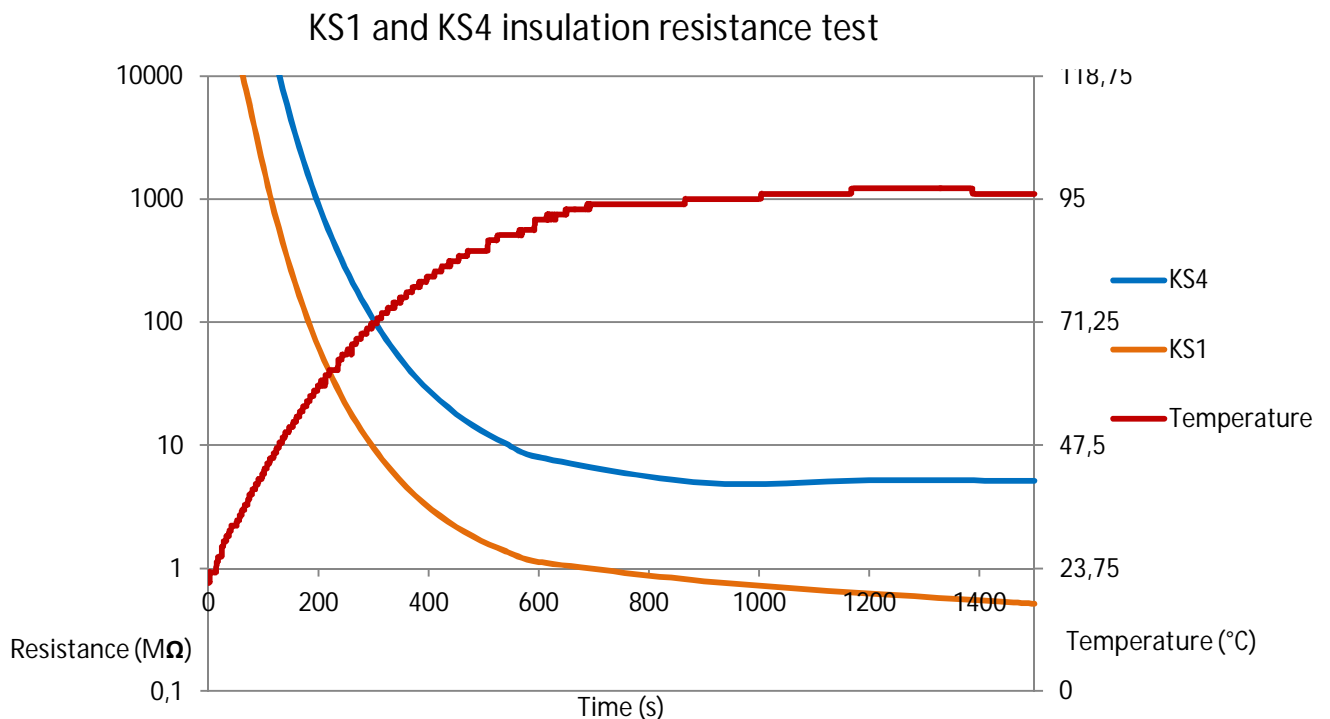


Figure 33 - Insulation resistance depending on temperature (sensors with old molding material)

Note that the lowest measured resistance for the KS1 model in Figure 33 is $516 \text{ k}\Omega$ and the lowest value for the KS4 is $5 \text{ M}\Omega$. It can be seen from the tests that all KS1 sensors from batch 11/5 **do not fulfil the specifications for $1 \text{ M}\Omega$ insulation resistance**. Already at around a temperature of $90 \text{ }^\circ\text{C}$ the insulation resistance drops below $1 \text{ M}\Omega$.

Note that the KS4 sensors with the new molding material are not included in this test.

3.7 Knock diagnostic system simulation

To be able to verify the behaviour due to changing insulation resistances a model of the knock sensor diagnostic system was created. The circuit was created and simulated with LTspice 5.

3.7.1 Knock sensor replacement circuit

The replacement circuit (Figure 24) for the knock sensor was inserted in the simulation with specified component values to get as realistic simulation results as possible.

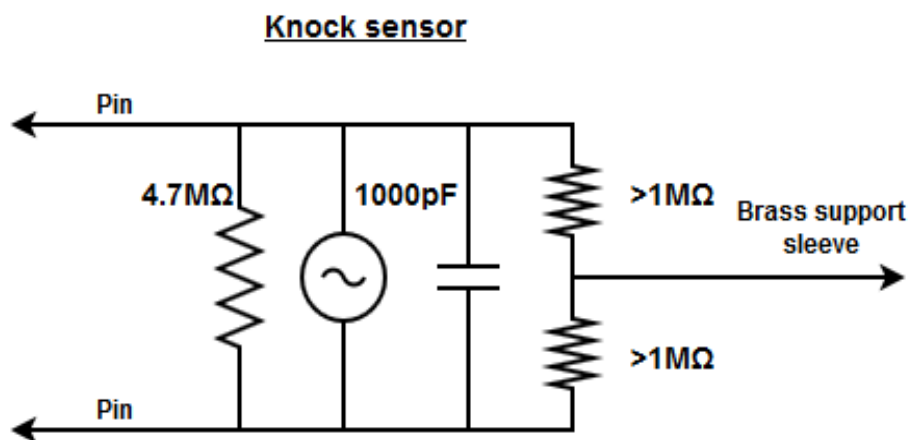


Figure 23 - Knock sensor replacement circuit

3.7.2 Simulation results

The same diagnostic voltage levels as in chapter 3.4 *KS1 heat test with WECS 8000* are now also reached when simulating the diagnostic output voltage with LTspice.

Figure 25 shows a simulation of a cold sensor with good insulation resistance.



Figure 24 - Diagnostic voltage when a “good” sensor is simulated

It is now verified that the output is the same as in real tests with wecsplorer. The results can be compared to the heat tests in chapter 3.4 *KS1 heat test with WECS 8000* and chapter 3.5 *KS1 drying test* earlier in this document.

Values from chapter 3.6 *insulation resistance tests* are used in the next simulation. The results can be seen in figure 27. The values are from an 11/5 dated KS1 sensor, when the sensor was heated to 95 °C.

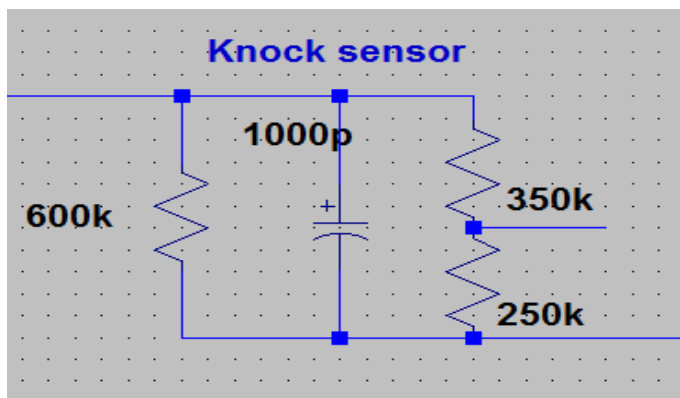


Figure 25 - Knock sensor replacement circuit in simulation model

With a shunt resistor at 600 k Ω and a pin to support sleeve resistance at 350 k Ω and 250 k Ω , figure 27 shows that the voltage output is the same as the real values from chapter 3.4 *KS1 heat test with WECS 8000*.



Figure 26 - Diagnostic voltage when a "bad" sensor is simulated

Based on these results the simulation model can be concluded to correspond well with the real characteristics of the knock sensor diagnostic system. This simulation can therefore be used in the future to find out the diagnostic voltage output from a sensor, if insulating resistances for the sensor are available.

3.8 Engine block potential influence

As mentioned earlier the bad insulation resistance of heated knock sensors is causing rising diagnostic values in the knock sensor diagnostic system. This is leading to that the possible **difference in the engine block potential** compared to the minus potential of the power supply, is causing current leaking in to the sensors increasing or decreasing the diagnostic value.

The dropping diagnostic values at the customer ship are caused because the engine block potential is more negative than minus the on power supply. When the sensors are warming up and the insulation resistance decreases, the negative voltage is causing a current to start leaking through the poor insulation resistance, beginning to interfere with the knock sensor diagnostic system.

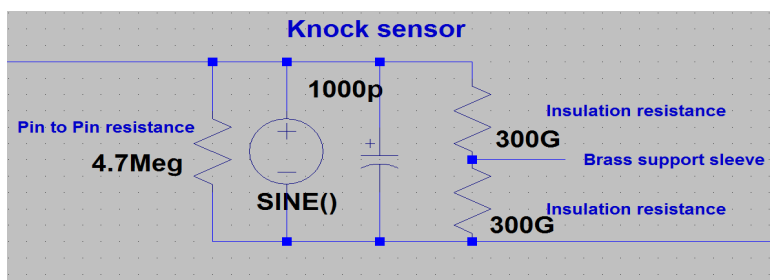


Figure 27- Knock sensor schematic

This has been confirmed by building a model of the whole diagnostic system in LTspice, where it is possible to achieve the same voltage levels when using this knock sensor model and the earlier measured insulation resistances.

It is confirmed by Bosch that the **molding material** on the knock sensors gets a lower resistance when heated. The degree of humidity in the molding material affects how low the resistance will go. A heat stabilizer based on metal salts is used in the molding material. Humidity dissolves these metal salts and the resulting solution with ions additionally decreases the insulation resistance.

In **figure 29** there are three examples of how different engine potentials can affect the diagnostic system:

1. Brass support sleeve **not** connected to ground => the measuring voltage 10V DC is causing a current leakage directly to the other pin via both the internal resistance of the piezomaterial and via the insulation materials, causing rising diagnostic levels.
2. Brass support sleeve connected to engine ground, ground and – (minus) on power supply have the same potential => the diagnostic value doesn't rise or drop remarkably.
3. Brass support sleeve connected to engine ground, ground and – (minus) on power supply **not** having the same potential => if for example the brass support sleeve has got a more negative potential than – (minus) on power supply (in this test -10 V), a current will leak from the brass support sleeve due to the bad insulation resistance into the heated sensor and cause the measured voltage to drop (Seri Balqis).

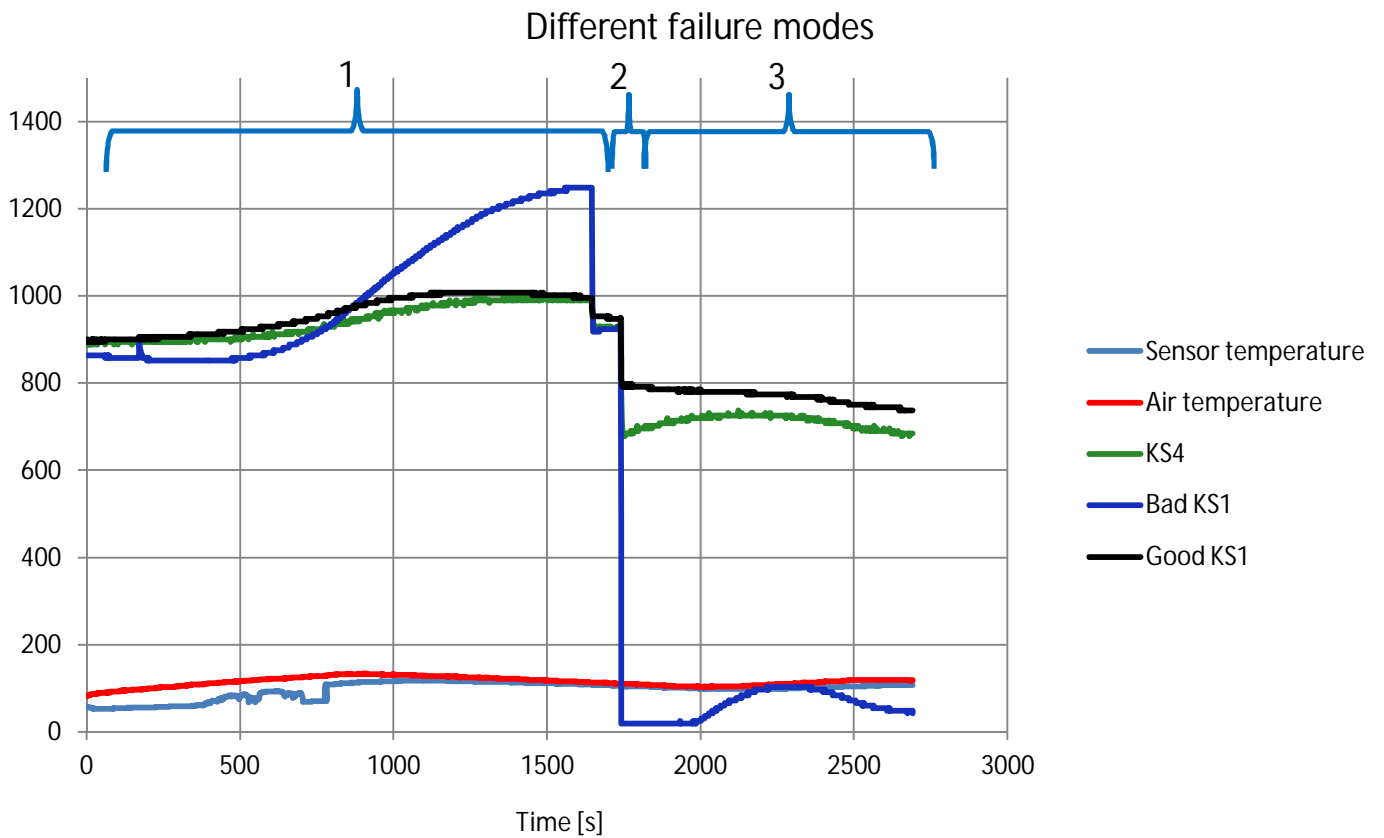


Figure 28 - Different types of failure modes on diagnostic voltage

3.9 Engine block potential tests

3.9.1 WECS 8000

3.9.2 UNIC C3

3.9.3 UNIC 2

3.10 Vibration tests

3.10.1 WECS 8000

3.10.2 UNIC C3

3.10.3 UNIC 2

4 Root Cause Analysis

A root cause analysis was performed to obtain a holistic view of the problem. The description of how the Root cause analysis process is done is documented in chapter *Root cause analysis theory*.

4.1 Incident report

Knock sensor diagnostic failure system

Report Date: 02-17-2015

Start Date: 08-01-2014

I. Problem Definition

What: Sensor failure alarm, knock sensor /load reduction

When: After changing to new KS-1 sensors

Where: 50DF WECS 8000 Ships

Significance: Sensors need to be replaced

Environment:

II. Report Summary

The root cause analysis resulted in a solved problem. Bosch is committed to making a new type of knock sensor which meets our requirements. The bad sensors on the affected ships will be replaced with this new type.

III. Solutions

Causes	Solutions	Solution Owner	Due Date
Molding material sensitive to moisture	Change to Bosch KS4 sensor model with new molding material	Dahl Thomas	02-17-2015

IV. Team Members

Name	Email	Member Info
Dahl Thomas		

V. Notes

1. Realitychart Status: The Realitychart and Incident Report have been finalized.
2. Rules Check Status: Missing Causes Resolved.
3. Rules Check Status: Conjunctions Resolved.

VI. References

1. Engine block potential influence tests
2. Insulation resistance tests

4.2 Reality Charting Possible Solutions Report

In the following table all possible solutions are listed. Only one solution passed the criteria check in the program. This solution is *Change to Bosch KS4 sensor model with new molding material*.

Causes	Solutions	Criteria Check	Implement	Solution Owner	Due Date
Too low insulation resistance in some sensor batches	Change to other sensors instead of Bosch	Failed	No		
Molding material sensitive to moisture	Change to Bosch KS4 sensor model with new molding material	Passed	Yes		
Pyroelectric effect	Change to non piezoelectric sensors	Failed	No		
KSFD-card	Redesign KSFD-card	Failed	No		

failure					
Voltage potentials in engine block affects the failure detection system	Create KSFD-card which is not sensitive to potential differences	Failed	No		
Minus terminal on power supply not connected to engine ground	Connect minus terminal on power supply to ground	Failed	No		
Brass support sleeve on knock sensor placed on engine block	Potential compensation	Passed	No		

1.1 Realitychart

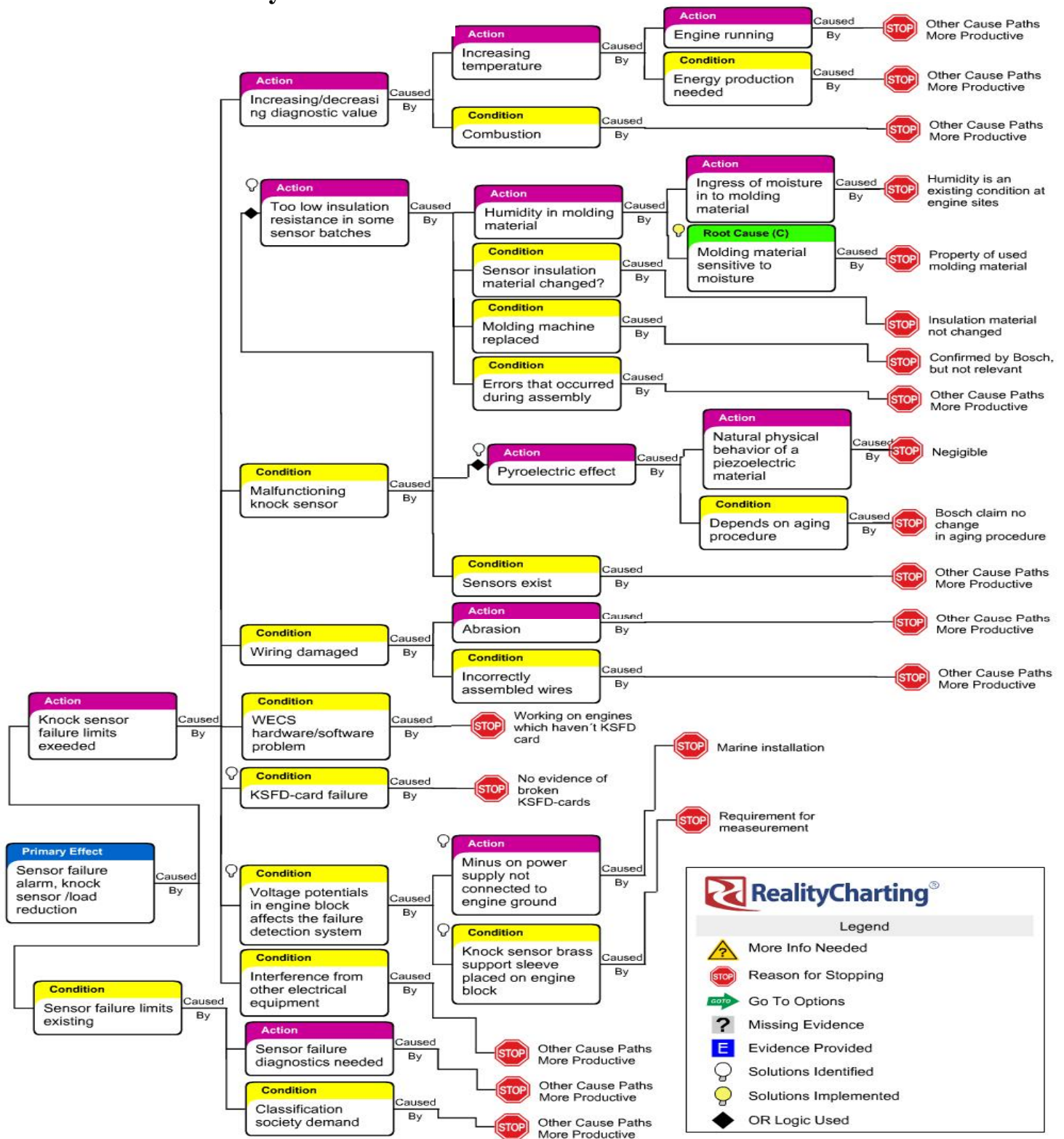


Figure 29 - Realitychart describing the problem

Figure 38 shows the Realitychart for the root cause analysis. The condition *Molding material sensitive to moisture* resulted in to become the root cause.

5 Results

The result of this thesis is mainly the knowledge of what is causing the rising/dropping knock sensor diagnostic voltage, i.e. the knock sensor insulation resistance. As a result of this knowledge I have had discussions with a knock sensor developer at Bosch, and with him put together a new knock sensor model that Bosch will start to manufacture.

The main cause of this problem, which also the root cause analysis showed, is the molding material on the knock sensors. The molding material on the KS1 sensor and the standard KS4 sensor consists of a metal salt-based heat stabilizer. The ingress of moisture into the molding material combined with the metal salts cause a significant decrease of the resistance in the molding material when it is heated up. Drying tests were performed with results that looked promising at the start, sensors can be dried and the dried sensors do have a higher insulation resistance. But after storage at room temperature for a few weeks the sensors will regain their initial insulation resistances.

All tests of the knock sensor diagnostic voltage shows one common factor: the KS1 sensors are very sensitive to temperature and voltage influences. Also in the insulation resistance tests the KS1 sensors show very bad results, meaning that not a single one of the KS1 sensors meets the insulation resistance specifications on $>1 \text{ M}\Omega$ at $95 \text{ }^\circ\text{C}$. Discussions have been held with Bosch regarding this issue, but no guarantee that the KS1 sensors will fulfil the specified values has been given. Uneven quality between sensor batches is also a problem with this sensor type.

Therefore samples of the newer KS4 knock sensor were ordered. This model proves to have a better insulation resistance than the KS1 sensor and shows more stable vibration signals than the KS1 sensors. Why this model exhibits higher insulation resistance than the KS1 model is unclear, the molding material in the sensors is after all the same. Even if the tests have shown better insulation resistance on the KS4 sensors we can see that different batches of this model also differ from each other. This is a bit worrying, the worst KS4 sensors in the *WECS 8000 -10 volt tests* show diagnostic values very near the *sensor failure low limit (500 mV)*.

An order specification was created for the KS4 sensor to be able to order sensors for field testing. Sensors have been sent for field testing to *a customer ship* but no results have been received within the timetable for this thesis work.

Further discussions were held with Bosch about how to find a solution for the insulation resistance problem. Bosch then revealed that they had recently developed a new molding material. Samples of a KS4 knock sensor with this new molding material were ordered of this model for testing. Testing results show that this model shows a remarkably higher insulation resistance than sensors with the old molding material.

Unfortunately this sensor model had a steel support sleeve instead of a brass support sleeve and silver plated contacts instead of gold plated. The steel support sleeve results in a slightly less sensitive sensor, but this would maybe not be a problem. Experience in the company concerning silver plated contacts on sensors says on the contrary that silver plated contacts are not a good solution on an engine. Therefore, further discussions were held with Bosch, which will result in a future creation of a new knock sensor model which matches our requirements on a knock sensor. This new knock sensor will be a new version of the KS4 sensor model and will consist of:

- The new molding material
- Brass support sleeve
- Gold plated contacts
- Jetronic connector
- Sonox P8 piezo disc.

Further field testing focusing on the frequency response of the KS4 sensor will still be needed to confirm that the sensors are suitable. If the results of this field test show that this sensor is suitable, this sensor model will also be used as the standard solution for new engines in production.

A replacement circuit for a knock sensor and a model for the whole knock sensor failure diagnostic circuit were built on order to be able to simulate how the system would respond to different insulation resistances, with no need to test sensors in a rig.

6 Discussion

The testing procedures in this thesis have required a lot of time, but without these tests it would have been quite hard to find the cause of the problem. The fact that Wärtsilä has had this problem on their gas engines now for over 10 years maybe supports that.

Afterwards the problem may seem simple, when it is solved, but it required a lot of work by me and my colleagues at Wärtsilä until the problem was finally solved. The pyroelectric effect was suspected to cause the rising diagnostic voltages for a long time until it was clear that it is the bad insulation resistance in the molding material that is causing the high voltage levels.

The problem also required full understanding of the piezoelectric/pyroelectric effect, which required a lot of studying. But now after I solved this problem I know that I am one of the persons that know most about knock sensors at Wärtsilä. I also spent a lot of time studying the knock detection systems for each control system in order to learn how they work.

Before starting with this thesis I also attended a Root Cause Analysis course at Wärtsilä in Turku in order to get the skills to perform a Root Cause Analysis on this knock sensor problem. A Root Cause Analysis does not solve the problem just like that, but by doing it I got an overall view of the problem and all the possible solutions. As a result it is easier to decide which solution is the best one. A lot of discussions have also been held with a knock sensor developer at Bosch, to get some help from him and his colleagues.

Further field-testing of the new sensors is needed to confirm that they are suitable for all gas engines. Defects and weaknesses which have been discovered in the knock-detection system during my tests and in regular operation of the engines will also be a future challenge.

Bibliography

- [1] *Overview* (Wärtsilä). [Online] <http://www.wartsila.com/en/about/company-management/overview> [visited 12.12.2014].
- [2] *Product Review W34SGD*. Tech. rep. Wärtsilä Finland. eprint: DBAD273877 (Wärtsilä IDM).
- [3] *Engine technology* (Wärtsilä). [Online] http://compass.wartsila.com/Operations/RD_and_design/engine_technology_activities/aut_control/Pages.aspx [visited 12.2.2015].
- [4] Holtti, J., 2012. *Tuning light knock limits on SG engine*. Bachelor's thesis in Automation technology. Novia University of Applied Sciences.
- [5] *Engine knocking*. [Online] http://en.wikipedia.org/wiki/Engine_knocking [visited 17.1.2015].
- [6] *Bosch Knock Sensors Overview, 2013*. Tech. rep. Bosch. (Bosch internal document).
- [7] *Piezoelectricity*. [Online] <http://en.wikipedia.org/wiki/Piezoelectricity> [visited 15.12.2014].
- [8] *Applications* (Piceramic). [Online] <http://piceramic.com/applications.html> [visited 15.12.2014].
- [9] *Fundamentals* (Piceramic). [Online] <http://piceramic.com/piezo-technology/fundamentals.html> [visited 15.12.2014].
- [10] *Polarization in Piezoceramic Materials* (Piezotechnologies). [Online] <http://www.piezotechnologies.com/Resources/White-Papers.aspx> [visited 15.12.2014].
- [11] Webster, J. G., 1999. *The measurement, instrumentation, and sensors handbook*. ISBN 978-0-8493-8347-2.
- [12] *Ferroelectric and Piezoelectric materials* (Zaahir Salam). [Online] <http://www.slideshare.net/researcher1234> [visited 15.12.2014].
- [13] *Knock Control v9.0 Application Description*. Tech. rep. Wärtsilä Finland. eprint: DBAB409026 (Wärtsilä IDM).

- [14] *Knock SF DC-method description*. Tech. rep. Wärtsilä Finland. eprint: DBAD233313 (Wärtsilä IDM).
- [15] *Root cause analysis*. [Online]
http://en.wikipedia.org/wiki/Root_cause_analysis
[visited 17.1.2015].
- [16] *RealityCharting-The standard for Effective Problem Solving*, 2010.
Apollonian Publications.
- [17] *Piezoelectric effect* [Online] <http://www.intechopen.com/books/advances-in-modern-woven-fabrics-technology/smart-woven-fabrics-in-renewable-energy-generation> [Visited 17.12.2014].